ACCSCIENCE PUBLISHING

International Journal of Bioprinting

REVIEW ARTICLE

3D-printed antimicrobial scaffolds for tissue repair: Intrinsic, stimuli-responsive, and topographical strategies

Zhixiang Nie[1,2,3†], Zihan Qu[1†], Shujing Wu[1], Yixuan Chen[1], Ke Li[1,2], Lanyang Liu[1], Yuhuai Liao[1], Zhiyao Zhang[1], and Yunsong Shi[1,2*]

[1]School of Stomatology, Tongji Medical College, Huazhong University of Science and Technology, Wuhan, Hubei, China

[2]State Key Laboratory of Materials Processing and Die & Mould Technology, School of Materials Science and Engineering, Huazhong University of Science and Technology, Wuhan, Hubei, China

[3]Engineering Research Center of Ceramic Materials for Additive Manufacturing, Ministry of Education, Wuhan, Hubei, China

Abstract

The restoration of tissue defects using 3D-printed medical implants enables precise anatomical matching and customizable microarchitectures. However, implant-associated infections and biofilm formation constitute persistent challenges, frequently compromising the efficacy of systemic antibiotic therapy and promoting drug resistance. In light of these limitations, the development of advanced 3D-printed implants endowed with localized, multifunctional antimicrobial properties has emerged as a critical clinical imperative. This review provides a systematic overview of recent progress in 3D-printed antimicrobial scaffolds, with current innovations classified into three principal synergistic strategies. The first strategy concerns implants fabricated from intrinsically antibacterial materials, which are further categorized into non-metallic systems (e.g., chitosan, antimicrobial peptides, and graphene oxide) and metal-based systems (e.g., silver, copper, zinc, magnesium, and metal–organic frameworks). These constructs provide continuous antimicrobial defense through the sustained release of bioactive ions or reactive oxygen species. The second strategy involves stimuli-responsive platforms that harness exogenous physical fields—such as photothermal, sonodynamic, or electrical stimulation—as well as endogenous biochemical cues (e.g., pH variations) to realize spatiotemporally regulated, on-demand bactericidal effects and to address infections located within deep tissue compartments. The third strategy capitalizes on structural and topographical micro-patterning that emulates bio-inspired architectures, thereby eliciting drug-free mechanobactericidal actions against adherent pathogens. Moreover, this review discusses key translational challenges, particularly balancing antimicrobial efficacy with the preservation of osteogenic activity and osseointegration, while addressing manufacturing complexities. By elucidating these mechanisms, this work provides forward-looking insights to inform the rational design and clinical translation of next-generation anti-infective medical scaffolds.

Keywords: 3D bioprinting; Antimicrobial scaffolds; Stimuli-responsive materials; Surface topography; Tissue engineering

†*These authors contributed equally to this work.*

***Corresponding author:**
Yunsong Shi
(shiyunsong@hust.edu.cn)

Citation: Nie Z, Qu Z, Wu S, *et al*. 3D-printed antimicrobial scaffolds for tissue repair: Intrinsic, stimuli-responsive, and topographical strategies. *Int J Bioprint.* doi: 10.36922/IJB026230232

Received: April 23, 2026

Revised: June 4, 2026

Accepted: June 23, 2026

Published online: July 24, 2026

1. Introduction

In recent years, three-dimensional (3D) printing—also referred to as additive manufacturing (AM)—has provided a diverse array of effective strategies for the management of tissue defects. By facilitating the production of patient-specific, anatomically conforming constructs, 3D printing enables precise control over macro- and microstructural parameters, including tunable porosity, pore dimensions, and surface topography.[1,2]

Despite these structural advances, implant-associated and surgical site infections persist as a formidable clinical obstacle. Studies indicate that microbial contamination occurs in up to 65% of open fracture wounds.[3] The pathogenesis of these infections is primarily driven by rapid bacterial adhesion and the subsequent formation of dense biofilms on the implant surface. This resilient physical barrier severely limits the local bioavailability of conventional systemic antibiotics, frequently necessitating supra-therapeutic regimens that carry considerable risk of systemic toxicity and promote the emergence of multidrug-resistant strains.[4] Consequently, the integration of intrinsic, localized antimicrobial functionalities into 3D-printed bone implants represents a promising direction to proactively mitigate infection risks, reduce systemic side effects, and concurrently support optimal bone regeneration.[5]

To address this challenge, current innovations in antimicrobial 3D printing strategies for bone tissue engineering converge on three synergistic paradigms (Figure 1, Table 1):

(i) Intrinsic antibacterial materials: Harnessing biomaterials with innate bactericidal activity—such as inherently antimicrobial polymers (e.g., chitosan [CS] and antimicrobial peptides [AMPs][6]), carbon-derived nanomaterials (e.g., graphene oxide [GO][7]), bioactive metals (e.g., silver [Ag],[8,9] copper [Cu], zinc [Zn],[10,11] and magnesium [Mg]), and metal–organic frameworks (MOFs)—to deliver sustained antimicrobial effects without sacrificing printability or long-term biocompatibility.

(ii) Stimuli-responsive systems: Developing scaffolds that trigger on-demand spatiotemporally controlled antimicrobial actions in response to exogenous physical fields (e.g., photothermal/photodynamic irradiation[12,13], ultrasound (US),[14,15] and mechanical/electrical stress[16,17]) or endogenous microenvironmental shifts (e.g., pH and reactive oxygen species [ROS]), enabling dynamic and precise infection eradication.

(iii) Biomimetic and topographical microstructuring: Emulating bio-inspired micro- and nano-architectures—such as the mechanobactericidal nanopillars of insect wings or the hierarchical textures of lotus leaves—to physically disrupt bacterial membranes and minimize attachment sites, providing a durable, drug-free bactericidal mechanism.

Existing reviews on antimicrobial 3D-printed implants have primarily focused on single intrinsic antibacterial agents or individual therapeutic modalities. In contrast, the present review uniquely proposes a broader conceptual framework that systematically integrates intrinsic antibacterial systems, stimuli-responsive platforms, and structural/topographical antibacterial strategies into a unified anti-infective paradigm. In addition to comprehensively summarizing these diverse approaches, this review further highlights the emerging realization of synergistic antibacterial strategies and critically evaluates the underlying bactericidal mechanisms within complex bone infection microenvironments.

Importantly, beyond antibacterial functionality alone, this review introduces a fabrication-oriented perspective by examining the printability of diverse antimicrobial agents and discussing how specific AM strategies can be optimized to preserve antibacterial activity and biological performance. Furthermore, comparative evaluations of the different antibacterial paradigms are conducted with respect to translational potential, manufacturing complexity, long-term biosafety, and the delicate balance between antibacterial efficacy and osseointegration. By aligning material innovation with pressing clinical needs, this analysis aims to provide forward-looking perspectives for the rational design and clinical translation of next-generation anti-infective implants for bone regeneration.

2. Intrinsic antibacterial materials

Intrinsic antibacterial materials represent the first line of defense in the design of anti-infective 3D-printed scaffolds. Unlike conventional bioinert scaffolds that rely on post-fabrication surface coatings or the physical encapsulation of traditional antibiotics, these materials inherently possess bactericidal or bacteriostatic properties within their bulk chemical structure. This inherent bioactivity allows them to be directly formulated into printable bioinks, thermoplastic filaments, or metallic powders. Consequently, the antimicrobial efficacy is seamlessly integrated throughout the entire macro- and micro-architecture of the scaffold, providing a continuous and durable defense against bacterial colonization even as the scaffold degrades or remodels over time.

In this section, we systematically review the recent advancements in 3D-printed scaffolds fabricated from these intrinsic antibacterial materials (Figure 2).

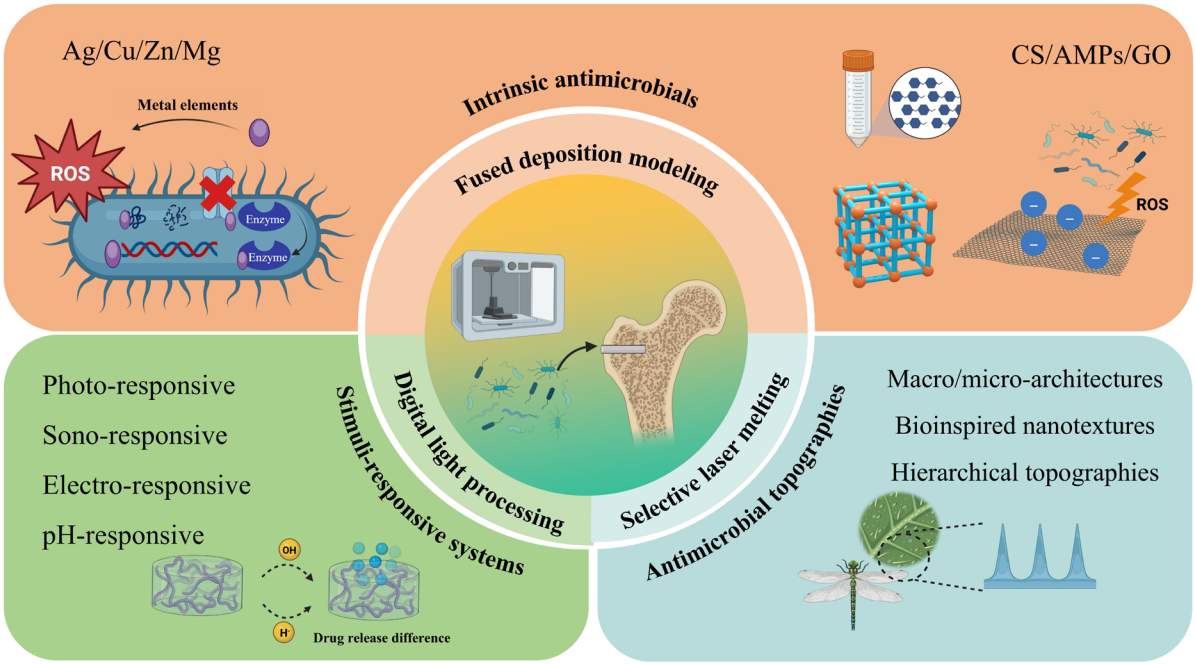

Figure 1. Schematic overview of the three primary antimicrobial paradigms in the design of 3D-printed scaffolds. Schematic created with BioRender. Chen, A. (2026) https://BioRender.com/a1hr9nr
Abbreviations: AMP: antimicrobial peptide; CS: Chitosan; GO: Graphene oxide; ROS: Reactive oxygen species.

Table 1. Comparison of Intrinsic, stimuli-responsive, and topographical antimicrobial strategies in 3D-printed scaffolds

Antimicrobial strategy	Activation mode	Advantages	Limitations	Clinical translation potential
Intrinsic systems	Passive, sustained antibacterial activity	Long-term activity; simple fabrication	Cytotoxicity; burst release; limited controllability	High
Stimuli-responsive systems	On-demand activation via external/internal stimuli	Spatiotemporal control; reduced systemic toxicity	Dependence on external triggers; high system complexity	Moderate
Topographical systems	Physical antibacterial action via surface micro/nanostructures	Drug-free mechanism; low resistance risk; structural stability	Limited mature biofilm eradication; complex nanofabrication	Emerging

Ultimately, the successful deployment of these intrinsic systems hinges on establishing a delicate balance between maximizing bactericidal efficacy and mitigating long-term mammalian cytotoxicity.

2.1. Non-metallic scaffolds

2.1.1. Chitosan

Chitosan, a natural cationic polymer derived from the deacetylation of chitin, exhibits intrinsic antibacterial properties and is readily amenable to chemical modification. Amino groups of CS are readily protonated under acidic conditions, forming positively charged polycations that exhibit intrinsic bactericidal activity. These polycations interact electrostatically with negatively charged bacterial cell membranes, resulting in the disruption of membrane integrity and the induction of cell lysis through cytoplasmic leakage.[18] In addition, low-molecular-weight CS (L-CS) can penetrate bacterial cell membranes and interact with intracellular constituents, leading to the disruption of bacterial metabolic processes and enhanced bactericidal

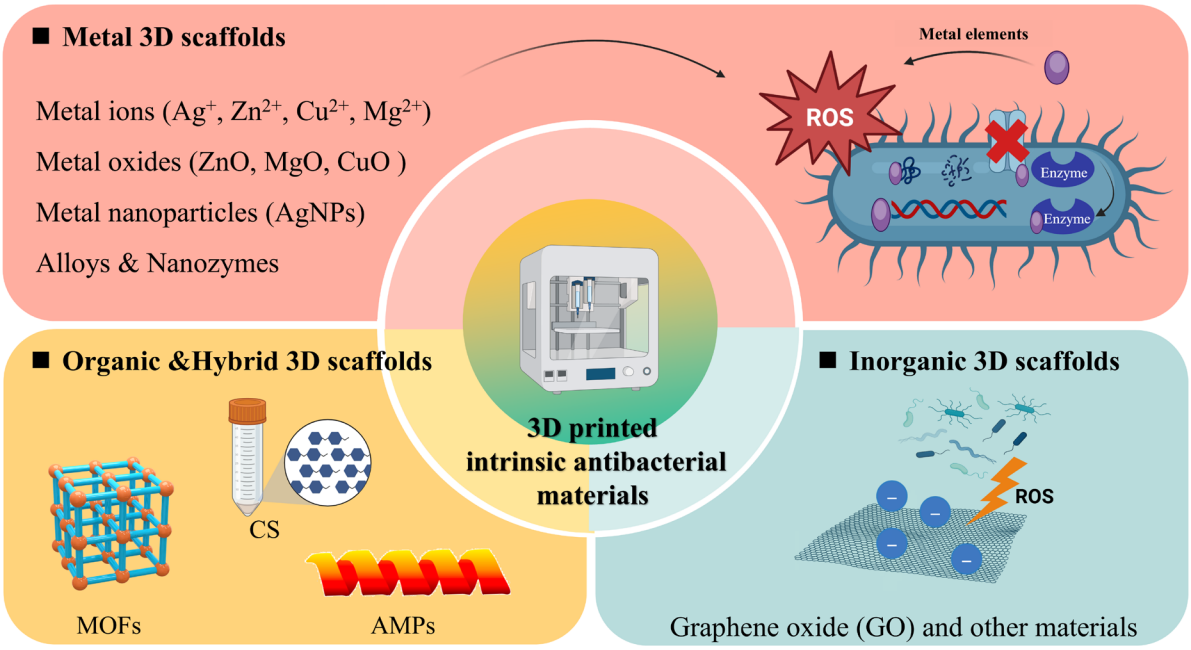

Figure 2. Schematic illustration of 3D-printed scaffolds incorporating intrinsic antibacterial materials, depicting key components and sustained antimicrobial mechanisms. Schematic created with BioRender. Chen, A. (2026) https://BioRender.com/d1wo567
Abbreviations: AMP: antimicrobial peptide; CS: Chitosan; MOF: Metal–organic framework; ROS: Reactive oxygen species.

activity.[19] Furthermore, the amino and hydroxyl groups present on CS molecules are capable of chelating metal cations, contributing synergistically to their antibacterial effects.

Due to its excellent biocompatibility and osteoconductivity, pure CS is widely utilized in bone and periodontal tissue engineering. It shows pronounced antibacterial activity against *Staphylococcus aureus* and *Escherichia coli*.[20] Furthermore, CS has shown promise in periodontal tissue engineering by promoting tissue regeneration while suppressing periodontal pathogens such as *Porphyromonas gingivalis*. However, the direct application of pure CS in 3D printing remains highly challenging. Its relatively low viscosity and inadequate rheological behavior limit printing fidelity, while slow crosslinking kinetics often lead to structural collapse during fabrication. In addition, the requirement for acidic printing conditions and the poor mechanical strength of pure CS further restrict the fabrication of complex multilayered architectures.[21]

To improve mechanical performance and broaden the functional versatility of CS-based scaffolds, current studies have primarily focused on three modification strategies: physical blending, surface coating, and chemical modification. First, physical blending and crosslinking within polymeric matrices can significantly enhance both the mechanical properties and antibacterial performance of CS. Reinforcing materials such as hydroxyapatite (HA), polylactic acid (PLA), GO, and graphene have been incorporated into CS matrices.[22] During the crosslinking process, both the molecular weight of CS and the type of crosslinking agent can markedly influence scaffold formation and physicochemical performance. Studies have shown that L-CS and medium-molecular-weight CS (M-CS) hydrogels crosslinked with 1% glutaraldehyde exhibited maximum swelling behavior at pH 2.0. Compared with L-CS hydrogels, M-CS hydrogels demonstrated greater thermal stability and a higher compressive modulus. In contrast, degradation studies conducted in both enzymatic and non-enzymatic media revealed a higher degradation rate for L-CS hydrogels.[23]

Beyond physical blending, CS-based coatings have been extensively applied in regenerative scaffold engineering. Zhao *et al.* developed a 3D-printed Ti–Nb alloy mesh scaffold coated with a semipermeable CS/gelatin/doxycycline layer via electrophoretic deposition technology.[20] Antibacterial zone inhibition assays and scanning electron microscopy analyses confirmed that the coating effectively inhibited *S. aureus* infection. Alternatively, chemical modification of the CS backbone offers another robust strategy to optimize its performance. Modified CS derivatives, such as quaternized CS (hydroxypropyltrimethylammonium

chloride CS), grafted onto 3D-printed scaffolds composed of poly(lactide-co-glycolide) (PLGA) and HA, reduce bacterial adhesion and biofilm formation under both *in vitro* and *in vivo* conditions.[24]

Finally, the successful translation of these modified CS strategies relies heavily on the selection of appropriate 3D-printing techniques and bioink formulations. For example, Chen *et al.*[25] employed direct ink writing (DIW) to fabricate CS/halloysite nanotube (HNT) hydrogels with high resolution and complex architectures. Their findings highlighted that DIW imposes stringent rheological requirements, necessitating precise control over the CS/HNTs ratio to achieve a composite bioink with optimal shear-thinning behavior and structural self-supporting capabilities. Alongside DIW, techniques such as cryogenic 3D printing and fused deposition modeling (FDM) are increasingly adapted to process these advanced CS-based anti-infective formulations.

2.1.2. Antimicrobial peptides

Bacterial antibiotic resistance has become a critical global health challenge, rendering the identification of plant-, animal-, and bacteria-derived AMPs with broad-spectrum antibacterial activity particularly promising.[26,27] Compared with conventional antibiotics, AMPs offer several advantages, including structural diversity, a broad spectrum of activity, and a reduced likelihood of inducing microbial resistance—positioning them as attractive candidates for combating antibiotic-resistant infections.

As short polypeptides (typically 20–50 amino acids) that exhibit potent activity against Gram-positive and Gram-negative bacteria, fungi, and certain viruses, AMPs have attracted increasing research attention in recent years. These peptides typically adopt four major structural motifs: α-helical, β-sheet, coiled-coil, and extended/disordered conformations. Their antimicrobial activity is largely attributed to the amphiphilic and cationic nature of AMPs, which facilitates transmembrane ion-channel formation and thereby disrupts bacterial membrane integrity. AMPs can also traverse bacterial membranes and directly engage intracellular targets, thereby exerting antibacterial activity (Figure 3).

In the realm of AM, AMPs can be directly incorporated into the scaffold matrix via bulk incorporation. However, their practical application is frequently hindered by high production costs, poor acid stability, susceptibility to *in vivo* proteolytic degradation, and short circulation half-lives.[28] Crucially, from a fabrication perspective, AMPs are notoriously difficult to process. Because their bactericidal mechanisms are highly folding-dependent, variations in the physicochemical microenvironment (e.g., pH fluctuations, high shear stress, or toxic crosslinkers) during bioink formulation can easily denature these peptides.[29] Furthermore, standard high-temperature extrusion processes would severely abrogate their biological activity. Achieving sustained, stable in vivo release while preserving peptide conformation thus remains a primary manufacturing hurdle.

To enhance the stability and long-term efficacy of AMPs within 3D-printed constructs, various biochemical modifications have been employed, including *D*-amino acid substitution, glycosylation, fatty acid conjugation, and nano-self-assembly. These strategies significantly enhance the chemical stability of AMPs against proteolysis.[28] Among natural AMPs, LL-37 (consisting of 37 amino acid residues) is extensively investigated in 3D-printing applications.[30] To deliberately circumvent the thermal degradation of LL-37, researchers have fabricated PLGA/β-tricalcium phosphate (TCP) composite scaffolds using low-temperature (cryogenic) 3D-printing technology.[31] Studies verified that scaffolds with high LL-37 loadings exhibited robust in vitro antibacterial effects against both *S. aureus* and *E. coli*, along with stable, sustained peptide release in a rat model of infected bone defects. Importantly, these constructs successfully eradicated local infections without inhibiting the proliferation of rat bone marrow mesenchymal stem cells, achieving a critical balance between antibacterial performance and osteogenic activity.

Alternatively, for inherently bioinert 3D-printed constructs (e.g., Ti-based or standard polymeric implants), antibacterial properties can be conferred through post-fabrication surface functionalization. For example, applying AMP-loaded hydrogel coatings via immersion allows for localized peptide delivery. Taking this concept further, recent innovations involve hydrogels encapsulating AMP-encoding plasmids, which facilitate sustained, *in situ* cellular expression and release of AMPs.[6]

2.1.3. Graphene oxide

Non-metallic nanomaterials, particularly GO, present a compelling alternative by combining robust antibacterial properties with enhanced biocompatibility. These materials operate through distinct mechanisms—including physical membrane disruption and ROS-mediated oxidative stress—that circumvent conventional resistance pathways. In 2010, the antimicrobial properties of graphene-based materials (GBMs) were first reported[32], which subsequently led to an increasing number of reports on the application of certain GBMs as antimicrobial nanomaterials.[33-35]

Researchers generally believe that the antimicrobial properties of GBMs are derived from the chemical and physical effects of direct contact between graphene flakes

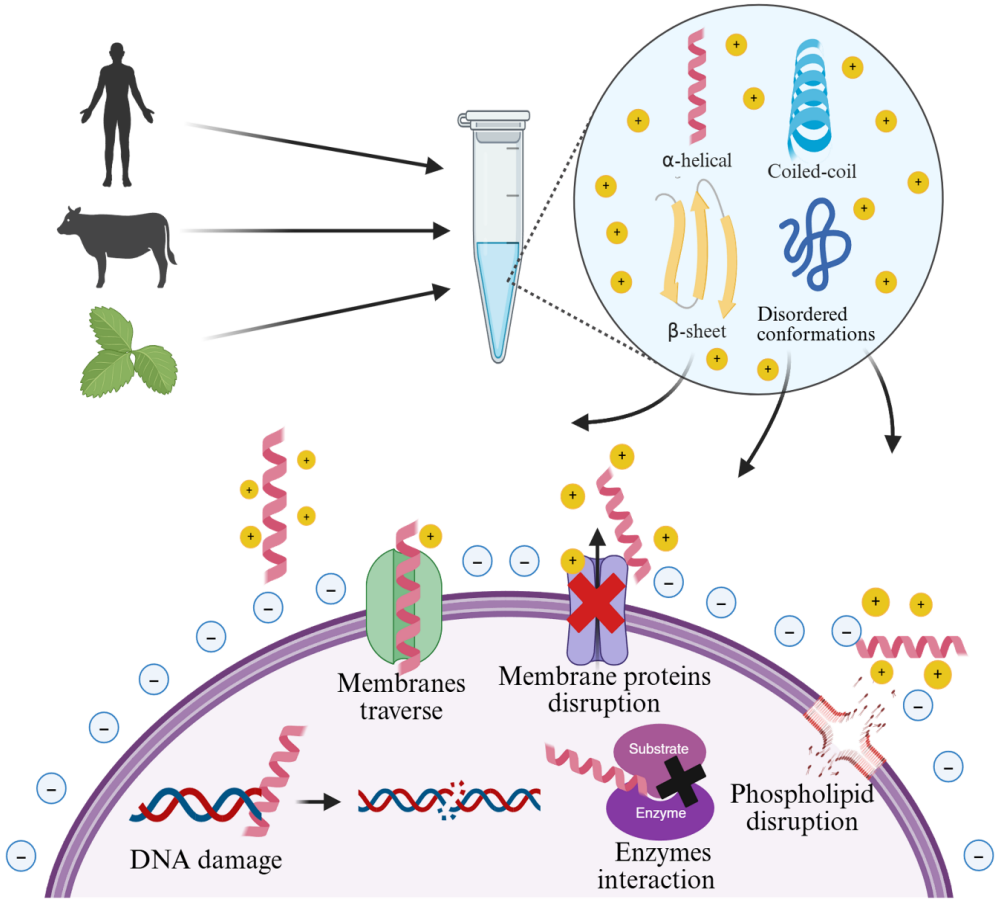

Figure 3. Comprehensive overview of antimicrobial peptides (AMPs): natural sources, structural diversity, and multifaceted bactericidal mechanisms. Schematic created with BioRender. Chen, A. (2026) https://BioRender.com/e4v9llz

and bacteria,[36,37] with the disruption of bacterial cell membranes being the primary target.[38] Specifically, these antimicrobial effects are primarily driven by graphene-induced oxidative stress and physical damage,[37,39] exhibiting time-dependent bactericidal kinetics that become significantly more pronounced with prolonged exposure (e.g., from several hours up to 24 h). At the micro-level, when bacteria are exposed to the material plane, electron transfer between GBMs and bacterial membranes[40] and O_2 adsorption by GBMs[35] lead to severe oxidative stress and subsequent bacterial death. Additionally, the sharp edges of GBMs can physically insert into the bacterial membrane, disrupting membrane-associated protein interactions and forming pores.[34,41] In 3D-printed thermally reduced GO (TrGO) constructs,[42] residual oxygen-containing groups (e.g., C=O and C–O) can increase surface hydrophilicity, thereby hindering the adhesion of bacteria with hydrophobic surfaces, while the material's remaining sharp and narrow surface asperities aid in bacterial detachment. However, it is important to note that the oxidation process of GO specifically usually leads to sharp-edge folding, thereby reducing the probability of physical membrane rupture. Consequently, the predominant antimicrobial mechanisms of action in most GO-containing scaffolds are ROS generation and oxidative stress caused by electronic destabilization.[43]

When selecting appropriate carbon nanomaterials for AM, material properties must be carefully balanced. Among GBMs, oxidized forms of graphite and graphene nanoplatelets have excellent bactericidal properties,[35,44] whereas GO is more biocompatible with mammalian cells due to its small size and high oxidation.[45] Therefore, GO and its derivatives are highly favored in the design of 3D-printed antimicrobial constructs. To maximize these antimicrobial effects, the orientation and exposure of GO flakes on the scaffold surface are crucial. In a pioneering study, Melo *et al.*[43] innovatively combined AM with non-solvent-induced phase separation (NIPS) technology. This

approach enabled effective incorporation of GO while ensuring sufficient flake exposure at the fiber surface. As a result, GO was effectively exposed on micrometer-scale AM polymer fibers, highlighting that process design can improve antimicrobial functionality while retaining the architectural advantages of 3D printing (Figure 4).

Furthermore, extending beyond bulk integration, GO can also be utilized for surface post-treatments; for instance, Ti-based implants coated with a GO–Zn/gelatin methacryloyl–phenylboronic acid (GelMA–PBA) layer via electrophoretic deposition not only successfully inhibited bacterial adhesion and biofilm formation but also enhanced the adhesion, proliferation, and differentiation of osteoblasts.[46]

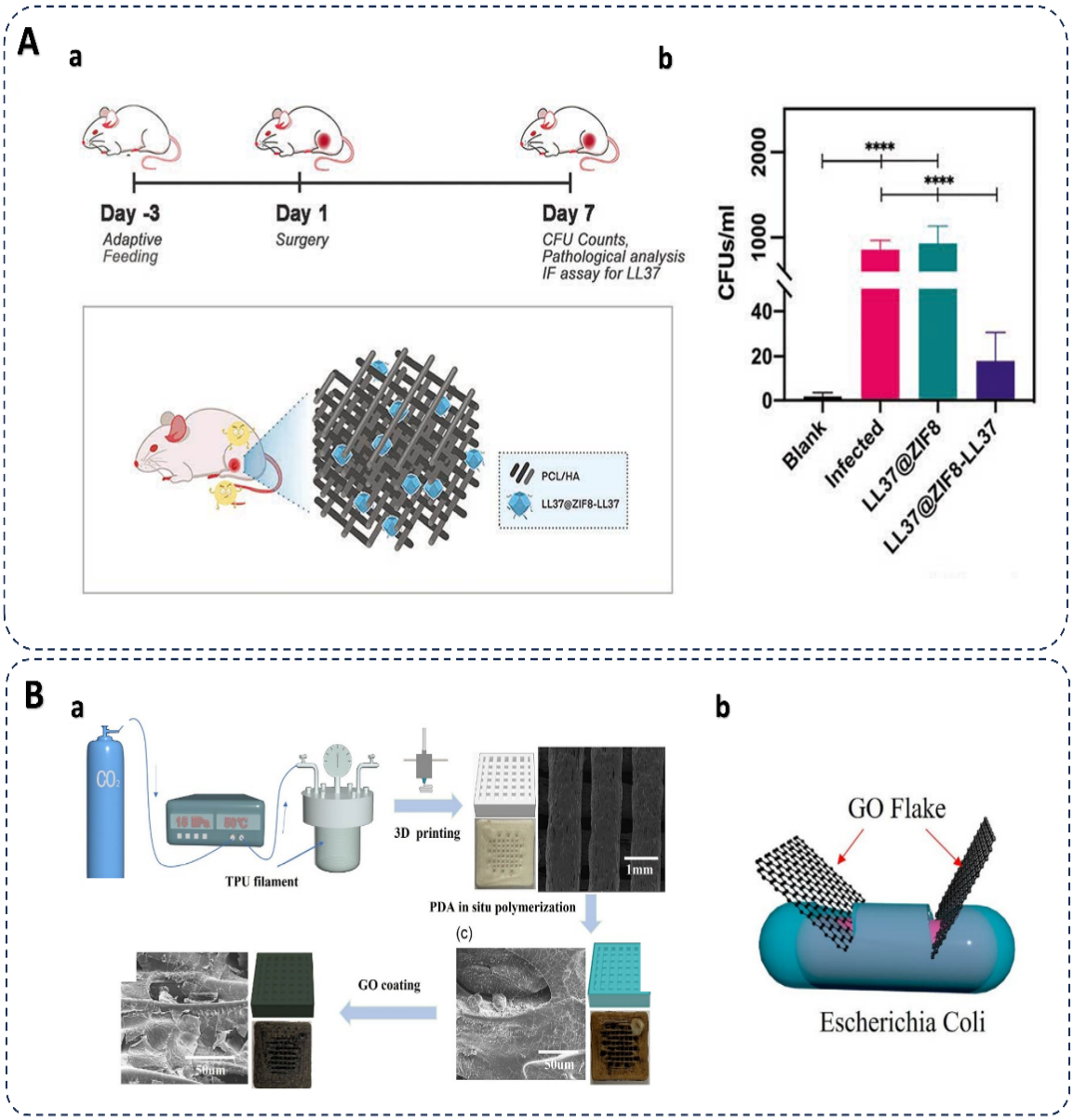

Figure 4. Representative non-metallic 3D-printed antimicrobial scaffolds featuring an antimicrobial peptide (AMP) and carbon-derived nanomaterials for tissue regeneration. (A) Schematic illustration and *in vivo* antibacterial efficacy of 3D-printed polycaprolactone/hydroxyapatite (PCL/HA) scaffolds loaded with LL37@ZIF8-LL37 nanoparticles. Reprinted with permission from Qu *et al.*[6] Copyright © 2022 Wiley-VCH GmbH. (B) Fabrication process and the contact-mediated "nano-knife" bactericidal mechanism of GO-coated hierarchical microcellular TPU scaffolds. Reprinted with permission from Zhang *et al.*[7] Copyright © 2022 Wiley-VCH GmbH.
Abbreviations: GO: Graphene oxide; PDA: Polydopamine; TPU: Thermoplastic polyurethane.

2.1.4. Synthetic antimicrobial polymers and plant-derived polyphenols

While CS, AMPs, and GO demonstrate promising antibacterial functionality in 3D-printed scaffolds, synthetic polymers—such as quaternary ammonium compound-modified polyesters—offer complementary advantages in processability and manufacturing adaptability. In photocurable resin systems used for stereolithography (SLA) or digital light processing (DLP), the incorporation of quaternary ammonium compounds may alter resin viscosity and partially attenuate ultraviolet (UV) light penetration, thereby requiring optimization of exposure parameters to maintain printing fidelity. In extrusion-based thermal printing processes such as FDM, these functional groups should possess sufficient thermal stability to withstand polymer melting and extrusion conditions without substantial degradation.

In parallel, plant-derived polyphenols such as tannic acid (TA) have attracted increasing attention for printable antibacterial scaffold fabrication. Owing to its abundant phenolic hydroxyl groups, TA can form dynamic hydrogen-bonding networks, thereby improving shear-thinning behavior and post-printing shape retention in DIW-based bioinks. In addition, TA can be introduced as a post-fabrication surface coating and has been reported to reduce *S. aureus* biofilm formation *in vitro*.[47] Furthermore, synthetic ionic liquids can be incorporated into printable inks, potentially conferring intrinsic contact-killing activity while simultaneously functioning as plasticizers to regulate rheological flow behavior.[40]

Notably, many intrinsically antibacterial non-metallic materials rely predominantly on contact-mediated antibacterial mechanisms, which may limit their efficacy against freely suspended planktonic bacteria compared with diffusible antimicrobial systems. To maximize this contact-dependent antibacterial activity, high-resolution AM can be leveraged to fabricate complex scaffold architectures with elevated surface-area-to-volume ratios, such as triply periodic minimal surface (TPMS) structures, thereby increasing the interaction interface between antibacterial surfaces and invading pathogens. Consequently, the integration of these multifunctional polymers into composite and multi-material scaffolds through advanced AM strategies is being increasingly explored for next-generation anti-infective bone implants.

2.2. Metal-based scaffolds

While the non-metallic scaffolds discussed in the previous section offer excellent printability and biocompatibility, their inherent mechanical limitations often restrict their use in load-bearing orthopedic and dental applications. To address this structural challenge, metal (e.g., Ag, Zn, Cu, Mg) and their corresponding metal oxide nanoparticles represent highly promising alternatives. Depending on the fabrication paradigm, these metallic agents can be integrated as active nanoparticles into composite bioinks or directly 3D-printed as monolithic load-bearing constructs, thereby coupling robust mechanical integrity with potent, broad-spectrum antibacterial activity. Consequently, Ag, Cu,[48,49] Zn, and Mg[50,51] have been extensively utilized as both bulk structural matrices and functional coatings in orthopedic implants.

The antibacterial mechanisms of metal and metal oxide nanoparticles are primarily attributed to their interactions with bacterial enzymes, thereby directly damaging cellular components such as DNA and proteins. Additionally, the generation of ROS induces severe oxidative stress in both Gram-positive and Gram-negative bacteria, ultimately leading to bacterial death (Figure 5). Furthermore, the antimicrobial efficacy of metallic materials can be significantly augmented through surface modification techniques, including plasma spraying, anodic oxidation, and chemical vapor deposition.[52,53] Simultaneously, nanotechnology-enabled micro/nanostructuring of metal surfaces[54] and advanced alloying strategies[55,56] further amplify their intrinsic antimicrobial properties while optimizing their biological safety profiles (Table 2).

Metal-based regenerative scaffolds are typically fabricated under high-temperature conditions using selective laser sintering (SLS)/selective laser melting (SLM) technologies. When compounding metal nanoparticles with polymeric or bioceramic inks for extrusion-based printing, achieving homogeneous nanoparticle dispersion is critical to prevent agglomeration and subsequent nozzle clogging. Conversely, for coated metallic implants, strengthening the interfacial bonding between the coating and the bulk substrate is essential to regulate corrosion kinetics and ensure a sustained, controlled release of antibacterial ions.[57] Crucially, a delicate equilibrium must be struck between bactericidal efficacy and host tissue cytotoxicity. According to ISO 10993-5, the standard for in vitro cytotoxicity, metal-based antibacterial scaffolds must maintain mammalian cell viability above 70% at the minimum effective ion concentration, while concurrently satisfying the genotoxicity and systemic safety requirements established by ISO 10993-3.

2.2.1. Silver

Silver, one of the most widely used antimicrobial metals, has been extensively utilized for scaffold surface

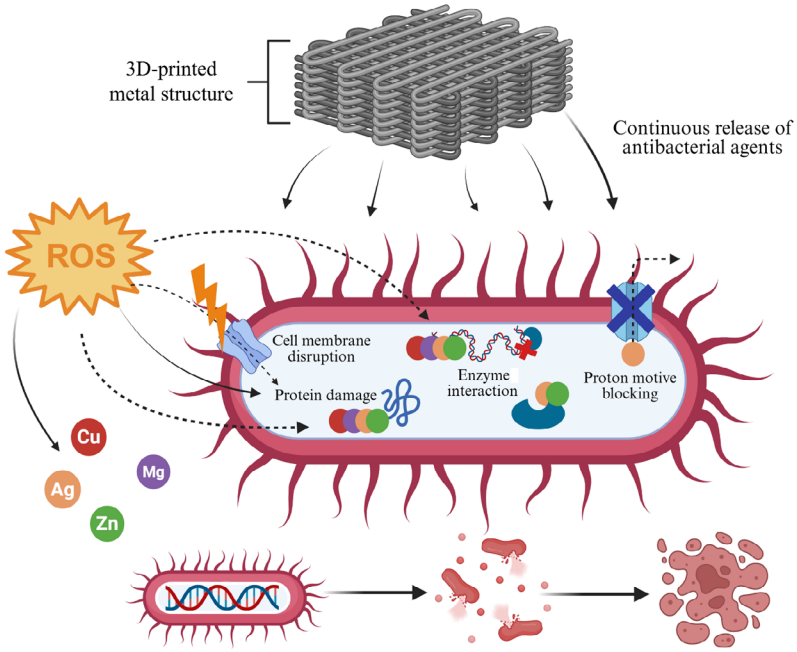

Figure 5. Schematic illustration of the antibacterial mechanisms associated with 3D-printed metal-based scaffolds. Schematic created with BioRender. Chen, A. (2026) https://BioRender.com/b1ufymx
Abbreviation: ROS: Reactive oxygen species.

Table 2. Summary of metals and metal nanoparticles utilized in 3D-printed implant scaffolds

Metal antibacterial agent	3D printing method	Scaffold materials	Incorporation strategy	Tested bacterial strains	Ref.
Ag	FFF	PLA + Cu	Bulk incorporation	*Staphylococcus aureus*, *Escherichia coli*	[58]
	Laser engineered net shaping	CPTi	Bulk incorporation	*S. aureus*, *Pseudomonas aeruginosa*	[59]
	SLM	Pure Ag	Monolithic scaffolds	*S. aureus*	[60]
	FFF	BG	Bulk incorporation	MRSA	[61]
Ag^+	SLM	316L stainless steel	Post-fabrication functionalization	*S. aureus*, *E. coli*	[62]
AgNPs	EBM	Ti6Al4V	Post-fabrication functionalization	*S. aureus*, *E. coli*	[63]
	EBM	Ti6Al4V	Post-fabrication functionalization	*S. aureus*, MRSA	[8]
	FDM	PCL	Post-fabrication functionalization	*S. aureus*	[64]
	EBM	Ti6Al4V	Post-fabrication functionalization	*S. aureus*, MRSA	[65]
	FDM	PEEK	Bulk incorporation	*S. aureus*, *E. coli*	[66]
	SLM	Ti6Al4V	Post-fabrication functionalization	*S. aureus*, MRSA	[67]

(*cont'd...*)

Table 2. (*Continued*)

Metal antibacterial agent	3D printing method	Scaffold materials	Incorporation strategy	Tested bacterial strains	Ref.
Cu	SLM	CoCrFeCuNi, high-entropy alloy	Bulk incorporation	*S. aureus*, *E. coli*	[68]
	DIW	GelMA	Bulk incorporation	MRSA, *E. coli*	[69]
Cu + Zn	LPBF	Zn-2Cu	Monolithic scaffolds	*S. aureus*, *E. coli*	[70]
Cu^{+} + Zn^{2+}	FDM	PLGA	Bulk incorporation	S. aureus	[71]
Mg	SLM	Mg–Nd–Zn–Zr	Bulk incorporation	MRSA, *E. coli*	[72]
Zn	FDM	Pure Zn	Monolithic scaffolds	*S. aureus*, *E. coli*	[73]
Zn + Ce	LPBF	Zn + Ce	Bulk incorporation	*E. coli*	[74]
Zn^{2+}	ETP	HA	Bulk incorporation	*S. aureus*	[75]
	FDM	PCL	Bulk incorporation	*S. aureus*, *E. coli*	[10]

Abbreviations: AgNP: Silver nanoparticle; BG: Bioactive glass; CPTi: Commercially pure titanium; DIW: Direct ink writing; EBM: Electron beam melting; ETP: Extrusion printing; FDM: Fused deposition modeling; FFF: Fused filament fabrication; GelMA: Gelatin methacryloyl; HA: Hydroxyapatite; LPBF: Laser powder bed fusion; MRSA: Methicillin-resistant *Staphylococcus aureus*; PCL: Polycaprolactone; PEEK: Polyetheretherketone; PLA: Polylactic acid; PLGA: Poly(lactide-co-glycolide); SLM: Selective laser melting.

functionalization[76] and as nanoparticles (AgNPs)[77] to confer antimicrobial properties to composites. This widespread application is attributed to its broad-spectrum antimicrobial activity[78-80] and acceptable cytocompatibility at appropriate doses.[81,82] Ag ions (Ag^{+}) have potent antimicrobial properties due to their ability to interfere with a variety of cellular processes. Research has demonstrated that Ag^{+} disrupts bacterial membrane integrity by binding to thiol (–SH)-containing membrane proteins, thereby increasing membrane permeability and triggering cytoplasmic leakage, ultimately leading to bacterial death.[83] Furthermore, Ag^{+} can penetrate bacterial cells and coordinate with electron-donor groups (e.g., thiols and phosphates) in DNA, RNA, and proteins, thereby impairing replication, transcription, and translation and inhibiting bacterial proliferation. In addition, Ag^{+} can promote excessive ROS generation, resulting in oxidative stress and multi-target cellular damage that further enhances bactericidal efficacy.[84] Ag is commonly incorporated into synthetic scaffolds (e.g., bioactive glass [BG] and porous stainless steel[62]) via ion doping or composite design to enhance its antimicrobial activity and biocompatibility. Marsh *et al.*[61] applied fused filament fabrication (FFF) to prepare a novel silicate bioactive and antimicrobial Ag-doped glass–ceramic (Ag-BG) scaffold and verified its strong inhibitory effect on Methicillin-resistant *S. aureus* (MRSA) colonization within the scaffold, indicating its potential for orthopedic applications (Figure 6).

For inherently bioinert implants, surface modification[85,86] is a widely adopted strategy to introduce Ag and endow implants with anti-infective performance.[87] Commonly used methods include plasma spraying,[88] magnetron sputtering,[89] sol-gel,[90] and micro-arc oxidation.[91] Vaithilingam *et al.*[92] and Vikulova *et al.*[93] applied Ag-based surface coatings to additively manufactured porous Ti-based implants to enhance antibacterial performance. A recent study by Liang *et al.*[94] showed that surface modification of CoCr alloys with Ag coatings is often the most effective method to reduce bacterial adhesion. However, Ag-coated implants face challenges regarding the durability of the antibacterial effect under wear. To address this issue, Maharubin *et al.*[59] directly printed Ti–Ag alloy-integrated implants via 3D printing, thereby eliminating post-fabrication surface-coating steps and potentially reducing manufacturing cost. The results suggested that the wear-associated antibacterial performance was comparable to that of coating-based approaches and was even slightly improved against Gram-negative bacteria.

Beyond metallic and ceramic matrices, Ag is increasingly incorporated into polymeric bio-scaffolds. While micro-scale metal/alloy fillers have been compounded with polymers (e.g., Alam *et al.*[58] fabricated antimicrobial scaffolds by compounding PLA with Cu, bronze, and Ag particles via FFF), AgNPs (1–100 nm) have emerged as the preferred additive for 3D printing. Given their high surface reactivity, AgNPs provide potent bactericidal activity without compromising the printability of the polymer matrix.[95] AgNPs can directly adsorb onto bacterial surfaces and compromise membrane integrity, facilitating nanoparticle internalization; concurrently, the sustained release of Ag^+ interacts with intracellular biomolecules to exert continuous bactericidal effects. Crucially, from a manufacturing perspective, achieving a homogeneous dispersion of AgNPs within the bioink is paramount. Nanoparticle agglomeration not only creates localized domains of compromised antibacterial efficacy but also profoundly alters ink rheology, leading to severe nozzle clogging during FDM extrusion or disruptive UV light scattering and compromised curing depth during SLA printing.[96]

Despite these excellent antimicrobial properties, given that high concentrations of Ag^+ may be biotoxic to mammalian cells, an important observation common to many experiments is that the degree of bacterial growth inhibition does not increase linearly with Ag^+ concentration.[59] The rate of inhibition increases gradually up to a threshold (e.g., ~1% Ag), and once above this level, the reduction of bacterial colonization is not significant. This suggests that future studies should more carefully evaluate the biocompatibility of Ag-containing materials and define an optimal/critical concentration window.

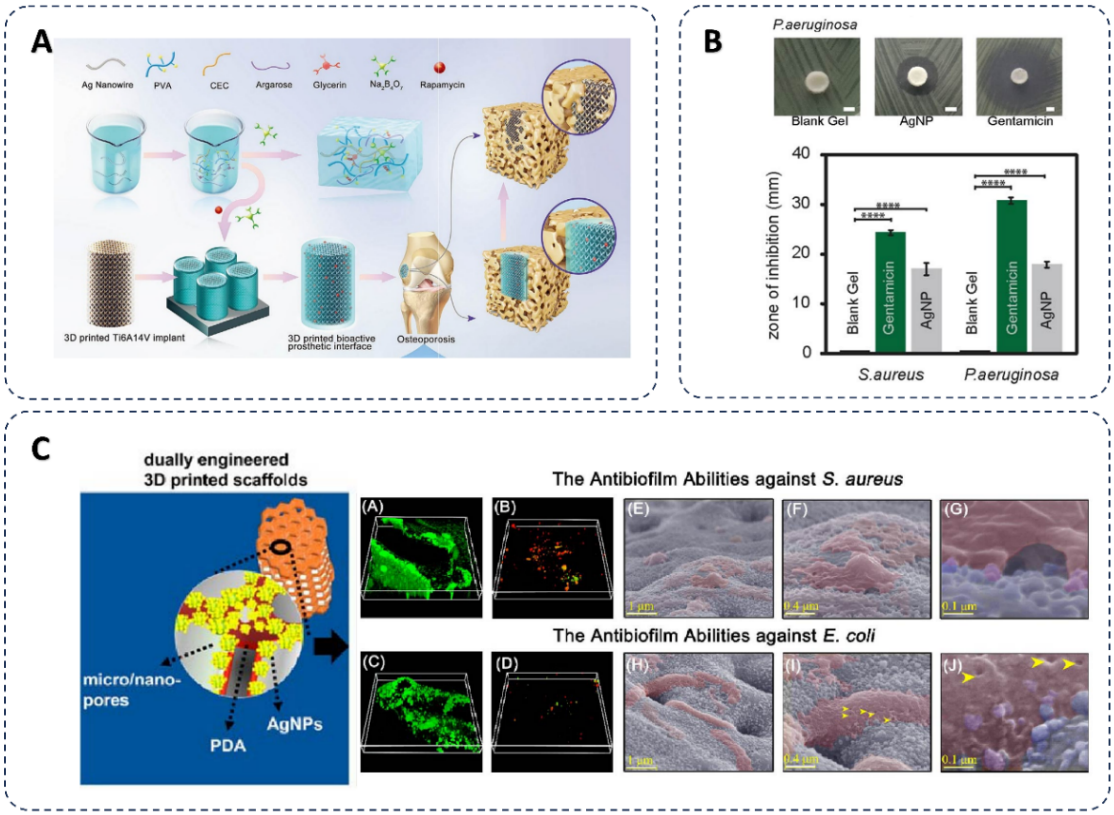

Figure 6. Representative 3D-printed antimicrobial scaffolds incorporating silver-based materials. (A) Schematic of 3D-printed porous titanium interfaces integrated with rapamycin and Ag nanowire-loaded hydrogels for osteoporotic osseointegration. Reprinted with permission from Li *et al.*[8] Copyright © 2022 Wiley-VCH GmbH. (B) Zone-of-inhibition assays demonstrating the antibacterial efficacy of 3D-printed hydrogels loaded with silver nanoparticles (AgNPs) or gentamicin. Reprinted with permission from Alizadehgiashi *et al.*[9] Copyright © 2021 American Chemical Society. (C) Dually engineered 3D-printed macroporous titanium scaffolds featuring PDA-assisted Ag-releasing surfaces for potent antibiofilm activity. Reprinted with permission from Jia *et al.*[63] Copyright © 2016 American Chemical Society.
Abbreviations: CEC: N-carboxyethyl chitosan; PDA: Polydopamine; PVA: Polyvinyl alcohol.

2.2.2. Copper

While Ag demonstrated remarkable broad-spectrum antimicrobial activity, its clinical translation is hindered by dose-dependent cytotoxicity and high material costs. These limitations have spurred interest in alternative metals, such as Cu. Cu offers comparable biocidal efficacy alongside distinct advantages, including significantly lower costs, enhanced osteogenic potential, and better long-term metabolic compatibility, making it a highly compelling candidate for a scalable 3D-printed orthopedic scaffold.

Copper has demonstrated antimicrobial properties against a variety of bacteria, including *S. aureus*[97] and *E. coli*,[98] and has been extensively used to modify different biomaterials for the treatment of implant-associated infections.[99] Incorporating Cu into mesoporous BG scaffolds, or introducing Cu–Zn nanoparticles into CS/nanoHA scaffolds, yields constructs that successfully couple antibacterial activity with osteoproliferative and osteogenic potential.[100] Emerging evidence also suggests that Cu-containing Ti alloys have excellent antimicrobial properties, reinforcing their viability as structural biomedical materials.[101,102]

Building upon Cu's intrinsic antimicrobial properties, recent studies have engineered Cu-based nanozymes (e.g., CuO, CuS) as emerging nanoscale biocatalysts.[103] These biomimetic systems enhance antibacterial efficacy through enzyme-like ROS generation—specifically via chemodynamic therapy (CDT)—while maintaining compatibility with 3D-printing workflows. Mechanistically, Cu-based nanozymes exhibit robust bactericidal properties by catalyzing the generation of highly toxic hydroxyl radicals (·OH) and concurrently depleting overexpressed glutathione within the bacterial microenvironment. Researchers have leveraged Cu-based redox platforms (e.g., CuO_2[104]) and integrated them with silica or BG templates to achieve localized, continuous oxidative bursts.

However, integrating these catalytic nanozymes into 3D-printing workflows presents unique manufacturing challenges. Within the Cu^{2+}/Cu^{+} redox cycle, the Cu^{+} state is highly unstable under mildly acidic microenvironmental conditions and is prone to disproportionation, resulting in an uncontrolled imbalance among Cu^{+}, Cu^{2+}, and CuO species. Crucially, from a fabrication perspective, this chemical instability is often exacerbated by the thermal stress or high-shear forces inherent in the 3D-printing process. To preserve catalytic activity and redox stability, researchers frequently resort to post-fabrication surface functionalization (e.g., immersion loading) or customized thermal stabilization strategies. For example, Shuai *et al.*[105] synthesized CuO_2/MoS_2 nanozymes using a low-temperature co-precipitation method to preserve their delicate initial state. To overcome the subsequent thermal challenges of integrating these nanozymes into poly-L-lactic acid (PLLA) scaffolds via SLS, they leveraged robust Cu–S–Mo interfacial sites. These unique interfacial structures successfully stabilized the copper atoms against thermal degradation during SLS melting and generated profound synergistic catalytic activity, achieving *in vitro* inhibition rates of 92.3% against *S. aureus* and 93.5% against *E. coli*.

2.2.3. Zinc

Zinc is a vital trace element that accelerates bone regeneration while exhibiting potent, broad-spectrum antibacterial activity, particularly against *S. aureus*. When exposed to physiological environments (*in vivo* and *in vitro*), Zn-based metals release Zn^{2+} through controlled corrosion. These cations are initially adsorbed onto negatively charged bacterial surfaces via Coulombic forces, interfering with cell-wall biosynthesis and compromising cell-wall integrity. Subsequently, Zn^{2+} can penetrate the cell wall, substitute for cationic positions on the cell membrane, and bind to intracellular proteins or anionic groups. This continuous ion infiltration disrupts membrane-associated metabolism and structural stability, ultimately leading to bacterial death[106] (Figure 7).

In 3D printing, the bactericidal efficacy of monolithic pure Zn constructs depends heavily on their topology. For example, FDM-printed porous scaffolds facilitate greater localized Zn^{2+} release than solid counterparts due to geometrically expanded specific surface areas.[73] When Zn is applied in antibacterial regenerative scaffolds, its concentration must be carefully controlled to balance infection eradication with tissue integration while minimizing cytotoxicity. Liu *et al.*[107] reported that Zn^{2+} at a concentration of 2.46 mg/L enhanced cell viability and promoted osteogenic differentiation, whereas concentrations ranging from 5.72 to 22.02 mg/L inhibited cell proliferation and impaired osteogenic differentiation. *In vivo* experiments further demonstrated that, after four weeks of implantation, the relatively high local Zn^{2+} concentration prevented direct integration between the Zn and the surrounding bone tissue.

Beyond pure metallic scaffolds, ZnO, a semiconducting metal oxide, has garnered significant attention due to its broad-spectrum antibacterial activity, antitumor activity, low toxicity, and unique piezoelectric properties. ZnO nanoparticles (ZnO-NPs) efficiently eradicate drug-resistant bacteria through combined membrane disruption, sustained Zn^{2+} release, and ROS generation. Taking advantage of its dual functionality, Chen *et al.*[108] utilized DLP 3D printing to incorporate ZnO-NPs into barium

titanate (BT) and HA scaffolds. The addition of ZnO-NPs not only provided intrinsic antimicrobial defense but also significantly enhanced the piezoelectric properties of the lead-free ceramic composite, paving the way for electro-responsive smart implants.

To further push the mechanical and therapeutic boundaries of Zn-based implants, alloying has become a particularly active area of research. Researchers frequently combine Zn with other bioactive metals (e.g., Zn–Cu[109] and Zn–Ag[74]) to achieve superior mechanical strength and synergistic antibacterial activity against MRSA. Notably, laser AM has been employed to alloy Zn with Ce, yielding porous Zn–Ce alloy scaffolds with significantly higher tensile strength and a vastly improved bacterial inhibition rate (81.36% vs. 34.28% for pure Zn).[74] The enhanced antimicrobial efficacy can be attributed to a synergistic contribution from Ce, which can coordinate with oxygen-containing functional groups and provide active sites for Zn^{2+} binding[109] and enhance their adsorption. Simultaneously, Ce ions actively increase bacterial cell membrane permeability[110,111] and catalyze local ROS production[112], thereby exponentially amplifying the overall antimicrobial performance of the 3D-printed alloy. Zn-based zeolitic imidazolate framework-8 (ZIF-8) MOF has emerged as a prominent candidate, serving as a highly effective and controlled reservoir of Zn^{2+}. ZIF-8 features a 3D porous structure, high specific surface area, excellent thermal stability, and sustained Zn^{2+} release during physiological degradation.[113,114] Demonstrated to exhibit potent antibacterial activity in wound healing and bone regeneration, ZIF-8 serves as a versatile antimicrobial platform.

2.2.4. Magnesium and other co-strategies

While Zn demonstrates strong antibacterial activity, its unpredictable degradation kinetics can limit its

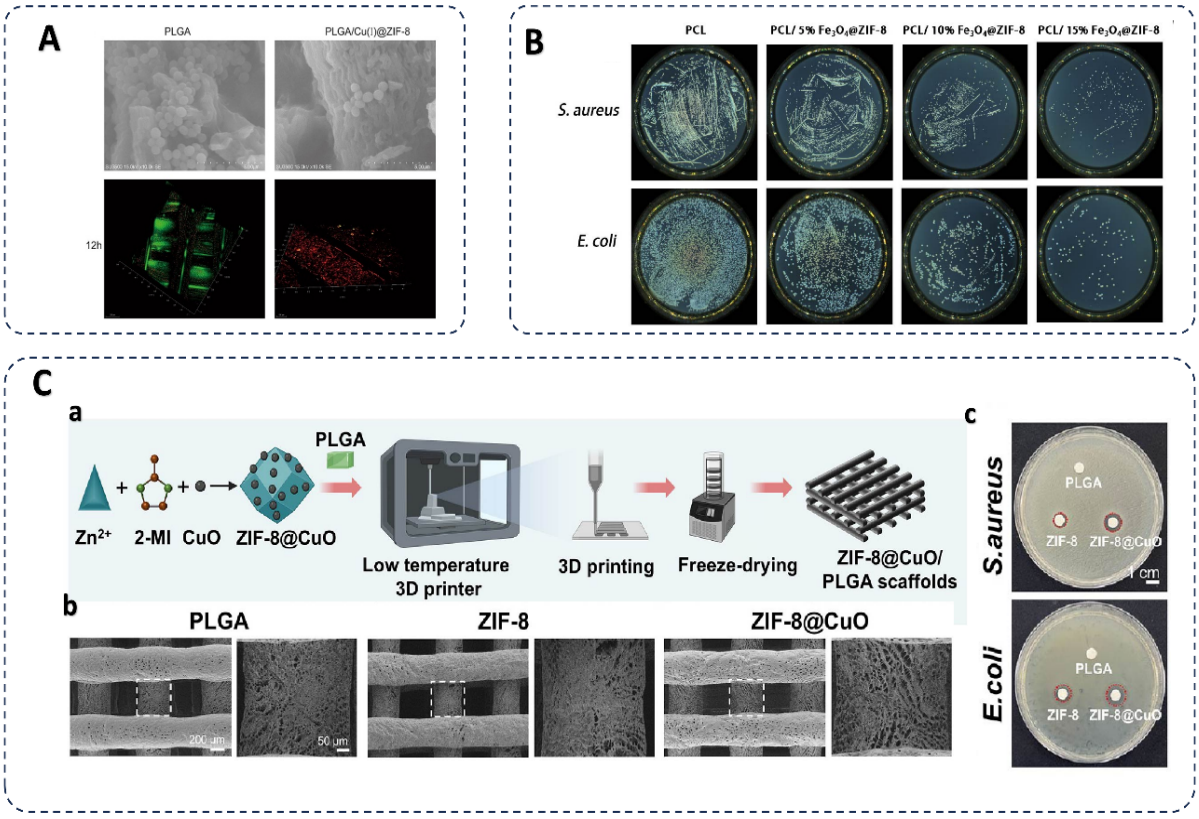

Figure 7. Representative zinc-incorporated antimicrobial strategies in 3D-printed architectures. Representative 3D-printed antimicrobial scaffolds incorporating zinc-based nanomaterials. (A) Fabrication of 3D-printed poly(lactide-co-glycolide) (PLGA) scaffolds containing Cu(I)@zeolitic imidazolate framework-8 (ZIF-8) nanoparticles that provide effective antibacterial and osteoconductive properties for infected bone repair. Reprinted from Zou *et al.*[71] (B) Development of 3D-printed magnetic polycaprolactone (PCL)/Fe_3O_4@ZIF-8 nanocomposite scaffolds that eliminate infection and promote new bone formation through the sustained release of zinc ions. Reprinted from Xiao *et al.*[10] (C) Design of intelligent responsive 3D-printed PLGA scaffolds integrating ZIF-8@CuO nanoparticles for pH/near-infrared (NIR)-triggered bacterial eradication and synergistic biomimetic bone regeneration. Reprinted with permission from Li *et al.*[11] Copyright © 2025 American Chemical Society.

clinical translation. These challenges have motivated the development of complementary approaches that utilize Mg as a co-strategy, offering distinct advantages. While Mg exhibits intrinsic antibacterial activity,[115,116] its superior osteoconductivity and more favorable degradation profile make it particularly suitable for orthopedic applications where bone regeneration is paramount.[117]

The bactericidal mechanism of Mg is unique among structural metals. Mg and its alloys have been demonstrated to possess broad-spectrum bactericidal ability driven by the localized alkaline environment generated during their degradation process. Specifically, the rapid increase in pH, coupled with elevated Mg^{2+} concentrations in the microenvironment, not only exerts direct bactericidal effects but also actively prevents the formation of biofilms by down-regulating the expression of biofilm-related genes in MRSA.

This complementary relationship between Zn (and other metals) and Mg underscores an emerging paradigm in antimicrobial biomaterials: rather than seeking single-element solutions, targeted combinations of metals can address specific clinical needs. Translating this concept into AM. Xie *et al.*[72] used SLM to fabricate a porous 3D-printed Mg–Nd–Zn–Zr alloy (denoted JDBM) with optimized mechanical properties for use as implants. Similarly, researchers proposed the addition of 1 wt.% MgO and 3 wt.% Cu to a commercially pure Ti (CP Ti) matrix, which was used as a coating on Ti6Al4V. This strategy successfully achieved an ~81% bactericidal efficacy after 72 h.

In summary, the high strength, durability, and tunable degradation profiles of metallic materials make them indispensable components of 3D-printed scaffolds, which are increasingly used in orthopedics, dentistry, and soft tissue restoration.[118-120] However, the use of metallic antibacterial agents is a double-edged sword, as they may provide robust bactericidal activity but inherently risk inducing cytotoxicity in mammalian cells. Accordingly, the use of standalone metallic materials, such as Ag or Cu, is somewhat limited, and their dosage is subject to rigorous *in vitro* and *in vivo* evaluation. Ultimately, the optimal design of next-generation implants relies on the intelligent integration of these metallic elements with the biocompatible non-metallic matrices discussed earlier, establishing a delicate balance between infection eradication and robust tissue integration.

3. Stimuli-responsive systems

While the intrinsic antibacterial materials discussed in Section 2 provide a robust and continuous baseline defense, their "always-on" nature can occasionally lead to the premature depletion of active agents or unintended long-term cytotoxicity. To address these limitations, recent research has increasingly focused on developing stimuli-responsive 3D-printed scaffolds (Table 3). These "smart" systems achieve enhanced, on-demand antibacterial activity via external or internal stimuli such as light, temperature, sound, and electricity.[121] By intelligently incorporating photothermal agents, employing photodynamic sensitizers to generate ROS, or using US and electrical stimulation to physically disrupt bacterial structures, these platforms offer highly programmable bactericidal interventions. Consequently, this strategy presents a promising route to mitigate clinical complications associated with severe bacterial inflammation, particularly in settings where antibiotic misuse has driven antimicrobial resistance.

Table 3. Summary of stimuli-responsive systems applied in 3D-printed implant scaffolds

Exogenous stimulus	Responsive material system	Fabrication & loading	Antimicrobial mechanism	Tested bacterial strains	Ref.
365 nm UV	AIEgen	SLA/Post-fabrication functionalization	PDT	*Staphylococcus aureus*, *Escherichia. coli*	[122]
1,064 nm NIR	CuS	FDM/Post-fabrication functionalization	PTT	*E. coli*	[123]
808 nm NIR	BPs	ETP/Post-fabrication functionalization	PTT	*S. aureus*, *E. coli*	[124]
	BPs	FDM/Post-fabrication functionalization	PTT	*S. aureus*, *E. coli*	[125]
	MXene	ETP/Bulk incorporation	PTT	*S. aureus*, *E. coli*	[41]
	Free carbon	ETP/Post-fabrication functionalization	PTT	*S. aureus*, *E. coli*	[126]
	AuNR	ETP/Bulk incorporation	PTT	*S. aureus*, *E. coli*	[12]
	CuO	ETP/Bulk incorporation	PTT/PDT/SDT	*S. aureus*, *E. coli*	[11]

(*cont'd...*)

Table 3. (*Continued*)

Exogenous stimulus	Responsive material system	Fabrication & loading	Antimicrobial mechanism	Tested bacterial strains	Ref.
565 nm LED light	TCPP	SLA/Bulk incorporation	PDT	*S. aureus*, *Pseudomonas aeruginosa*	[127]
	Porphyrinic MOF (PCN-224)	DLP/Bulk incorporation	PTT/PDT	*S. aureus*, *E. coli*	[128]
US	BT +Cu^{2+}	FDM/Post-fabrication functionalization	SDT/ CDT	*S. aureus*, *E. coli*	[14]
LIPUS	ZnO-NPs + BT	DLP/Bulk incorporation	SDT	*S. aureus*, *E. coli*	[108]
	MMBOx	ETP/Bulk incorporation	SDT/PDT	*S. aureus*, *E. coli*	[129]
Direct current	TrGO	FDM/Bulk incorporation	Electrophoretic anti-adhesion	*S. aureus*	[42]
Occlusal pressure	BCZT	DLP/Monolithic scaffolds	ROS	*S. aureus*, *Porphyromonas gingivalis*	[16]
pH	CaPNPs	ETP/Bulk incorporation	AMP	Wound pathogens	[130]
	CS	ETP/Bulk incorporation	Vancomycin	*S. aureus*	[131]

Abbreviations: AIEgen: Aggregation-induced emission-active luminogen; AMP: antimicrobial peptide; BCZT: Ba0.85Ca0.15Zr0.1Ti0.9O3; BPs: Black phosphorus nanosheets; BT: Barium titanate; DLP: Digital light processing; ETP: Extrusion printing; FDM: Fused deposition modeling; LED: Light-emitting diode; LIPUS: Low-intensity pulsed ultrasound; MMBOx: Magnesium- and manganese-doped bismuth oxide with oxygen vacancies nanoparticles; MOF: Metal–organic framework; NIR: Near-infrared; NP: Nanoparticle; NR: Nanorod; PDT: Photodynamic therapy; PTT: Photothermal therapy; ROS: Reactive oxygen species; SDT: Sonodynamic therapy; SLA: Stereolithography; TCPP: 5,10,15,20-(tetra-4-carboxyphenyl) porphyrin; TrGO: Thermally reduced graphene oxide; US: Ultrasound.

Most importantly, stimuli-responsive systems enable precise, *in situ*, and on-demand release profiles, allowing exquisite spatiotemporal control over antimicrobial action. This means that high-dose, localized bacterial eradication can be triggered exactly when an infection is detected, while simultaneously maintaining a safe, biocompatible microenvironment that actively supports osteogenic regeneration. Furthermore, electrically and mechanically responsive materials (e.g., piezoelectric scaffolds) have been shown to exhibit sustained, self-powered antimicrobial activity, rendering them promising candidates for next-generation biomedical applications (Figure 8).

3.1. Photo-responsive scaffolds

Phototherapy is regarded as a highly promising alternative approach for managing bacterial infections. The aim is to avert the clinical complications associated with the misuse of antibiotics, such as multidrug resistance and subsequent bacterial inflammation caused by therapeutically implanted scaffolds. Phototherapy encompasses two primary therapeutic modalities: photothermal therapy (PTT) and photodynamic therapy (PDT). By introducing photothermal agents or photodynamic agents into the 3D-scaffold microenvironment, potent antimicrobial properties can be elicited on demand. PTT involves the use of photothermal agents activated by NIR laser irradiation. These agents generate high localized temperatures, thereby disrupting the structure of bacterial cell membranes. This enhances the permeability of bacterial membranes and inhibits bacterial activity through thermal ablation, resulting in significant bactericidal effects.[132] For example, significant research has been conducted on incorporating free carbon into 3D-printed prosthetic scaffolds to induce photothermal antibacterial activity.[133,134] Similarly, Ti_3C_2 (MXenes), a new class of 2D transition-metal carbides with excellent photothermal conversion efficiency, have been explored as photo-responsive components. Researchers successfully applied 3D printing technology to synthesize GelMA/β-TCP/sodium alginate (Sr^{2+})/MXene composite hydrogel scaffolds (GTAM), which demonstrated outstanding antimicrobial effects under 808 nm NIR irradiation.[41] However, heat shock proteins produced during the reaction process can increase bacterial thermotolerance, reducing the destructive impact of mild temperatures. Furthermore, the high heat generated by photothermal agents has the potential to compromise the health of periwound host tissues, limiting the uncontrolled application of PTT in medical prosthetics (Figure 9).

As an alternative strategy, PDT has attracted considerable attention due to its minimal side effects and direct therapeutic efficacy.[135,136] PDT relies on photosensitizers to generate bactericidal singlet oxygen ($^1O_2$) and other ROS in the presence of light at specific wavelengths. These redox reactions result in irreversible damage to pathogenic bacteria, representing a potent modality for implant infections.[78,79] Commonly used photosensitizers include

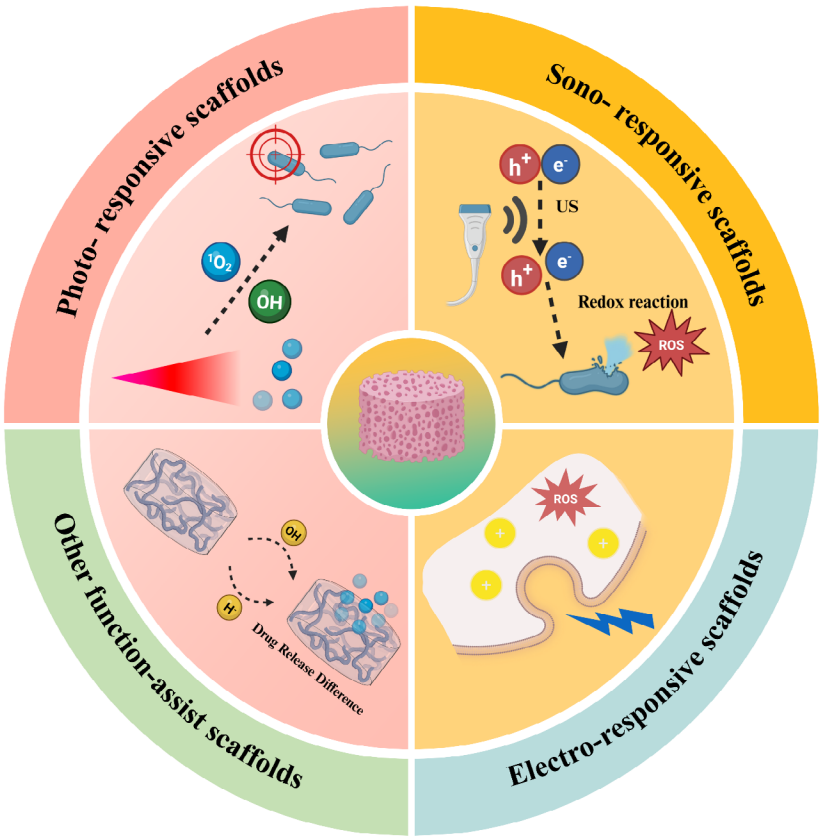

Figure 8. Schematic illustration of the stimuli-responsive 3D-printed antimicrobial scaffolds. Schematic created with BioRender. Chen, A. (2026) https://BioRender.com/h43ug3r

NIR dyes such as methylene blue (MB) and its derivatives. Additionally, amorphous N-doped carbon has emerged as a potential photosensitizer,[81] as confirmed by the Mn/hyaluronic acid-coated single-atom nanozyme (HSAE) scaffolds developed by Gao *et al.*[137]

Remarkably, recent advancements have seamlessly integrated PDT agents directly into the AM process. Several heterogeneous materials, including metal semiconductors,[91] carbon-based materials,[85] and upconversion nanoparticles,[86] have been utilized as photocatalysts for photo-controlled reversible deactivation radical polymerization (photo RDRP). Furthermore, some MOFs with light-trapping properties have been developed as dual-functional photocatalysts[138] for PDT,[139] CO_2 reduction, and the decomposition of water.[140] Specifically, 2D MOF nanosheets based on 5,10,15,20-(tetra-4-carboxyphenyl) porphyrin (TCPP) exhibit highly efficient light-trapping properties.[141] For example, Zhang *et al.*[127] utilized 2D ZnTCPP nanosheets as a photocatalyst for SLA 3D printing in an open-air environment. This approach not only yielded high-resolution 3D-printed objects but also exhibited robust antimicrobial activity against both Gram-positive and Gram-negative bacteria by generating photoactivated $^1O_2$. Beyond unimodal treatments, light-driven effects are increasingly synergized with other stimuli to produce multimodal antimicrobial mechanisms. For example, Li *et al.*[142] fabricated a 3D-printed hydrogel scaffold embedded with gallium–indium eutectic (EGaIn) liquid-metal microdroplets. This scaffold successfully eliminated bacterial infections by coupling the photothermal effect of liquid metal with US-assisted mechanical disruption.

In addition, the combination of PTT/PDT with CDT has been demonstrated to synergistically enhance the bactericidal effect. In the study by Huang *et al.*,[143] an MXene/CaO_2 bio-heterojunction (MC bio-HJ) was synthesized to amplify the bactericidal properties of PTT and PDT. This was achieved through the sustained release of Ca^{2+}, which sensitized bacterial cell membranes and increased their permeability, thereby exponentially enhancing ROS-mediated and thermal damage induced by PTT and PDT.

In comparison with traditional antimicrobial therapies

(e.g., systemic antibiotics or simple Ag^+ coatings), photo-triggered antimicrobial therapy offers several distinct advantages. Firstly, it provides rapid, on-demand bactericidal action. Secondly, it employs non-specific physical and oxidative damage mechanisms, making it highly efficient against both normal and multidrug-resistant pathogens.[144] However, their clinical translation hinges on overcoming specific AM challenges. Directly integrating photothermal or photodynamic agents into light-curing systems (e.g., SLA/DLP) often induces severe light scattering and attenuates UV penetration, compromising curing depth and printing fidelity. Balancing antimicrobial efficacy with structural precision requires optimizing printing parameters—such as exposure time—or employing post-fabrication surface coatings instead of bulk incorporation. Overcoming these manufacturing complexities enables photo-triggered platforms to combat antibiotic resistance while promoting localized tissue regeneration.

3.2. Sono-responsive scaffolds

The clinical utility of PDT in the management of infected bone defects is often constrained by the inadequate penetration of light into deep biological tissues. Conversely, sonodynamic therapy (SDT) overcomes this critical limitation by leveraging the tissue penetration advantage of US. The mechanism of action of US initially involves a significant increase in the permeability of bacterial cell membranes, leading to a reduction in membrane fluidity and depolarization. Beyond mechanical disruption, sonosensitizers utilize US energy to eradicate bacteria via two primary ROS-generating mechanisms: sonoluminescence and pyrolysis. The absorption of US energy triggers the separation of electron–hole pairs (e^-–h^+) within the sensitizers, leading to redox reactions.[145] Consequently, the abundant generation of ROS exerts potent antibacterial activity by causing bacterial lipid peroxidation, severe membrane disruption, and ultimately cell death. Furthermore, US irradiation can be employed

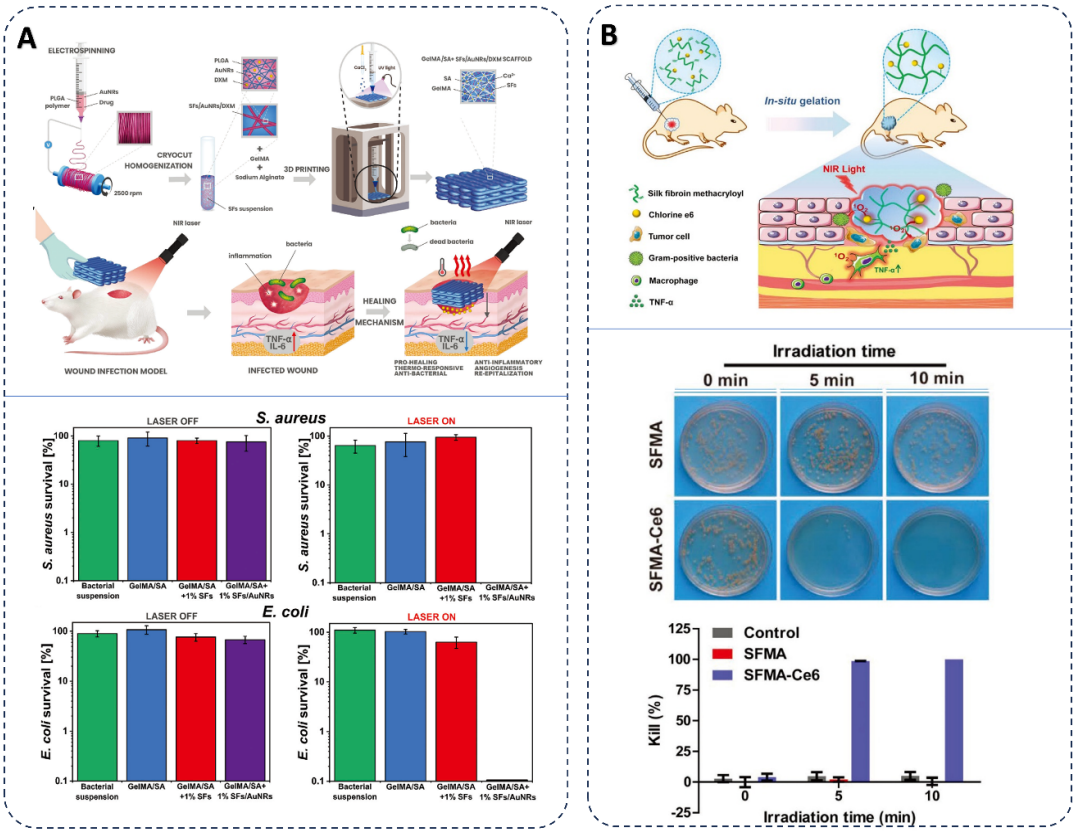

Figure 9. Representative photo-responsive 3D-printed antimicrobial scaffolds for advanced wound management. (A) A gelatin methacryloyl (GelMA)/sodium alginate (SA) hydrogel incorporating gold nanorod (AuNR)-loaded electrospun short filaments accelerates infected wound healing by eradicating *Staphylococcus aureus* and *Escherichia coli* via potent near-infrared (NIR)-activated photothermal therapy. Reprinted from Rybak *et al.*[12] (B) A dual-functional silk fibroin methacryloyl (SFMA)-Ce6 hydrogel scaffold utilizes NIR-activated photodynamic therapy to simultaneously suppress residual melanoma and promote the healing of *S. aureus*-infected wounds. Reprinted with permission from Tang *et al.*[13] Copyright © 2021 Wiley-VCH GmbH.

to enhance the localized delivery of drugs by mildly increasing local temperature to facilitate diffusion or by cleaving unstable chemical bonds within antimicrobial agents.

To further amplify these acoustic effects, exogenous US has been shown to powerfully promote the piezoelectric effect in lattice-asymmetric acoustic sensitizers. During SDT, US stimulation mechanically deforms the crystalline structure of these materials, generating built-in piezoelectric potentials and establishing an inherent electric field. This piezoelectric effect significantly enhances SDT by accelerating electron transfer, thereby amplifying ROS generation and bactericidal outcomes.[146] For example, highly printable piezoelectric materials include barium titanate ($BaTiO_3$), ferroelectric bismuth ferrite ($BiFeO_3$), and strontium titanate ($SrTiO_3$). However, integrating high concentrations of these dense, inorganic piezoceramic nanoparticles into polymeric bioinks introduces substantial manufacturing challenges. It drastically alters the rheological behavior of the inks, leading to increased shear viscosity, poor shape fidelity, and frequent nozzle clogging during extrusion-based 3D printing. Furthermore, for piezoelectric ceramic scaffolds fabricated via powder-based 3D printing and subsequent high-temperature sintering, a post-fabrication high-voltage poling process is critically required to align ferroelectric domains and unlock their piezoelectric potential. To further enhance their piezo-catalytic and antimicrobial properties, researchers have increasingly augmented these conventional sensitizers with metal or non-metal dopants, such as Al ions,[15] Se nanoparticles,[147] and Ag nanoparticles[148] (Figure 10).

Crucially for clinical translation, low-intensity US (LIU, power between 0.01 and 3 W/cm^2) is heavily preferred to minimize the risk of damaging surrounding healthy tissues. However, traditional acoustic sensitizers with high dielectric constants often fail to respond effectively to LIU. To overcome this barrier, Chen *et al.*[149] developed a novel piezoelectric-catalyzed bioheterojunction (P-bioHJ) consisting of a 2D BiOI photocatalyst, a thin layer of 2D MXene, and naringenin enriched with surface oxygen vacancies. By coating 3D-printed polyetherketoneketone (PEKK) scaffolds with this advanced material, they successfully enhanced charge separation and disrupted the bacterial respiratory chain via the acoustic cavitation effect, achieving highly efficient synergistic antimicrobial and osteogenic outcomes in deep tissue environments.

Moving beyond unimodal sonodynamic action, SDT has also been combined with CDT to produce a synergistically enhanced bactericidal effect.[137] In this multimodal approach, ultrasonic stimulation triggers transition-metal catalysts to efficiently catalyze the conversion of endogenous H_2O_2 into highly toxic hydroxyl radicals (·OH).[150,151] For example, a Cu-based transition-metal catalyst that undergoes a valence transition between Cu^+ and Cu^{2+} has been shown to induce Cu-toxicity-like death of bacteria while simultaneously promoting angiogenesis.[14] This CDT process subsequently synergizes with piezoelectric sonosensitizers to achieve explosive ROS generation. Recently, Sun *et al.*[129] developed a 3D-printed, ROS-logic-gated GelMA-PBA/poly(vinyl alcohol) (PVA)/MMBOx scaffold. Fabrication-wise, PVA pre-crosslinking significantly improved the bioink's extrusion stability. Under acidic conditions and US stimulation, the scaffold's piezoelectric-sonocatalytic activity achieved >96% clearance of *S. aureus* and *E. coli* biofilms (in vitro CFU and live/dead assays). Post-infection, it seamlessly transitioned to a ROS-scavenging mode to rejuvenate senescent stem cells and accelerate bone repair. Collectively, these responsive elements constitute a nanoscale reactor that can be seamlessly integrated into 3D-printed bone implant scaffolds, facilitating highly efficient infection eradication alongside robust bone defect repair.

3.3. Electro-responsive scaffolds

In recent years, the integration of 3D printing with electroactive biomaterials has enabled the development of highly precise, stimuli-responsive implants. The application of external electrical stimulation allows for precise spatiotemporal control over the amplitude, duration, and periodicity of the applied voltage.[152,153] The mechanisms by which direct current (DC) eradicates bacterial biofilms[154] are multifaceted. Primarily, DC alters bacterial electrophoretic migration by using electro-osmotic forces to push negatively charged bacteria away from the conducting surface, thereby achieving a robust anti-adhesion effect. Furthermore, the inter-electrode electric field can induce irreversible electroporation,[155] while localized electrolysis generates ROS and alters the microenvironmental pH.[156,157] Additionally, electron transfer processes at the material-tissue interface compromise bacterial membrane integrity, potentially triggering autolysis and cell disruption.[157] However, translating these DC-responsive mechanisms into 3D-printed scaffolds necessitates overcoming specific fabrication challenges. Ensuring uniform dispersion of conductive fillers (e.g., carbon nanomaterials or metal nanoparticles) within polymeric bioinks is critical; inadequate dispersion not only causes severe nozzle clogging during extrusion-based printing but also results in discontinuous internal electrical networks, thereby severely compromising overall electroporation efficacy.

While DC-responsive materials offer programmable antimicrobial effects, their reliance on external power

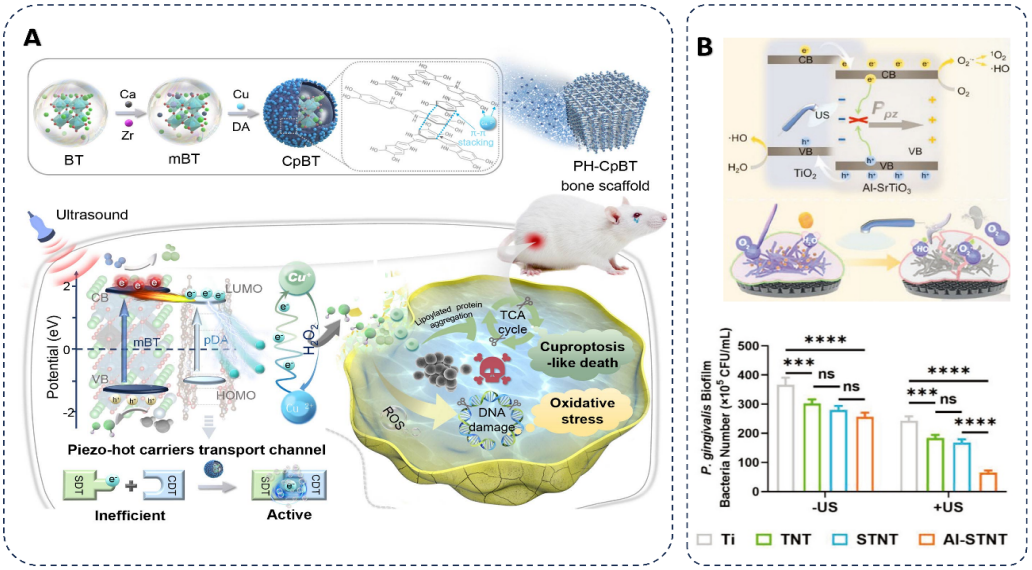

Figure 10. Representative ultrasound (US)-responsive antimicrobial strategies employing piezocatalysis and sonodynamic therapy. (A) Schematic illustration of a bone scaffold engineered with copper-armed barium titanate (CpBT) nanoreactors that eradicate *Staphylococcus aureus* biofilms through US-activated tandem catalysis and cuproptosis-like death. Reprinted from Huang *et al.*[14] (B) Mechanistic overview of an aluminum-doped strontium titanate/titanium dioxide nanotube (Al-STNT) coating that eradicates *Porphyromonas gingivalis* biofilms by triggering the piezoelectric effect under exogenous US to generate abundant reactive oxygen species (ROS). Reprinted with permission from Pan *et al.*[15] Copyright © 2024 Wiley-VCH GmbH.

sources and transcutaneous wires limits clinical practicality for deep orthopedic and dental implants. This limitation has motivated a paradigm shift toward self-powered electro-responsive systems, particularly piezoelectric materials and triboelectric nanogenerators (TENGs).[17,158] Piezoelectric materials are capable of converting physiological mechanical stresses (e.g., weight-bearing or joint movement) into built-in electric fields and antimicrobial surface potentials without the need for external batteries.[159,160] Among these, piezoceramics such as $BaTiO_3$ and organic polymers such as polyvinylidene difluoride (PVDF) are the most rigorously examined.[161] Because bulk piezoceramic scaffolds often lack intrinsic broad-spectrum bactericidal properties, they are frequently functionalized via 3D printing. For example, Chen *et al.*[16] utilized DLP to construct a novel piezoceramic scaffold combining $BaTiO_3$, HA, and ZnO-NPs. Pushing the boundaries of pure piezoceramics, recent breakthroughs have successfully utilized advanced AM to fabricate biocompatible piezoelectric $Ba_{0.85}Ca_{0.15}Zr_{0.1}Ti_{0.9}O_3$ dental implants. This pure piezoceramic architecture acts as a highly efficient, occlusion-activated autonomous system. It directly converts daily masticatory forces into a robust, localized built-in electric field, triggering non-Faradaic electron transfer and generating continuous intracellular ROS without compromising the implant's load-bearing structural integrity. Consequently, this self-activating mechanism profoundly disrupts the vital metabolic pathways of peri-implantitis-associated pathogens (e.g., *P. gingivalis* and *S. aureus*) while simultaneously providing necessary mechanical support and promoting osteogenesis. Similarly, ZIF-8 nanocrystals have been used to decorate PVDF foam, where the piezoelectric potential of PVDF actively regulates the release kinetics of Zn^{2+} from ZIF-8, achieving targeted metal-ion enrichment and synergistic antimicrobial efficacy.

Complementing these self-powered generators, exogenous conductive polymer composites offer excellent bioactivity and tunable electrical properties. These matrices are typically enhanced with carbon-based nanomaterials, such as graphene or its derivatives. For example, Angulo-Pineda *et al.*[42] developed a porous composite scaffold by incorporating electrically conductive, thermally reduced TrGO nanoparticles into a PCL matrix using 3D printing. The composite's distinct surface morphology and hydrophilic functional groups provided baseline antimicrobial resistance. Crucially, upon electrical stimulation, the bactericidal activity of the material was significantly enhanced, concurrently increasing adhesion, viability, and osteogenic differentiation of human stem cells (Figure 11).

3.4. pH-responsive scaffolds

Beyond exogenous physical triggers, endogenous biochemical cues—most notably pH—have emerged as

highly effective stimuli for on-demand antimicrobial delivery. Unlike intrinsic antimicrobial scaffolds, which rely on the passive, spontaneous, and sustained baseline diffusion of active agents (e.g., Ag^{+}, Zn^{2+}), stimuli-responsive platforms encapsulate these identical therapeutic payloads within smart matrices. Consequently, the release profile shifts from passive degradation to active, spatiotemporally gated actuation. Bacterial infections typically lower the local microenvironmental pH due to the accumulation of acidic metabolic byproducts. Alterations in this wound microenvironment yield precise stimuli capable of inducing the targeted release of antimicrobial agents, particularly from 3D-printed hydrogels.

At the molecular level, these pH-stimulated responses are typically accomplished by the incorporation of acid-labile linkages (e.g., imine and acylhydrazone bonds) or by the integration of acidic (sulfonic and carboxylic) and basic (amino) functional groups into the polymer backbone through free radical polymerization.

By translating these mechanisms into macroscopic 3D-printed architectures, Huang *et al.*[130] elegantly employed calcium phosphate nanoparticles (CaP NPs) as pH-responsive switches. By formulating and fabricating alginate-CaP nanocomposite scaffolds via 3D printing, they created a dynamic system that accelerates the release of encapsulated antimicrobial drugs at the acidic pH of infected wounds, while effectively attenuating the release at the physiological pH of healthy skin. This intelligent, self-regulating methodology significantly enhances the efficacy of wound infection treatments while actively mitigating the risk of antimicrobial toxicity to surrounding healthy tissue. Expanding this paradigm to hard-tissue infections, Lin *et al.*[131] developed a 3D-printed CS scaffold for osteomyelitis utilizing acid-labile Schiff base (imine) linkages. Fabrication-wise, this dynamic crosslinking endowed the bioink with excellent shear-thinning properties, enabling precise extrusion printing without toxic crosslinkers. In the acidic osteomyelitis microenvironment (pH 5.5), rapid imine bond cleavage triggers the on-demand release of vancomycin to eradicate *S. aureus*, whereas physiological pH robustly prevents premature burst release. This pH-gated profile actively shields local osteoblasts from drug toxicity, seamlessly integrating infection eradication with robust bone defect regeneration.

4. Structural and topographical antibacterial strategies

Conventional antimicrobial approaches face significant limitations, particularly regarding the unpredictable release kinetics of local antibiotics and the rampant development of bacterial resistance. Consequently, surface engineering via highly specific structural topographies (e.g., customized geometries, nanotextures, and hierarchical micro-nano architectures) has emerged as a compelling, drug-free strategy to physically reduce bacterial adhesion or achieve direct bactericidal effects.[162]

At the macro- and micro-scale, the architectural design of 3D-printed scaffolds fundamentally dictates bacterial behavior. Low-porosity scaffolds inherently suppress biofilm formation by restricting stable bacterial attachment sites and limiting nutrient permeation. For example, among TPMS designs, the Schwarz primitive structure with low porosity has been shown to significantly minimize *S. aureus* biofilm formation.[163] Moreover, utilizing Pickering emulsion inks as a 3D printing template followed by freeze-drying enables the precise fabrication of highly interconnected micro- and macroporous networks. In this specific hierarchical configuration, macropores facilitate mammalian cell infiltration and nutrient transport, while micropores restrict bacterial motility.[164] Furthermore, the impact of surface roughness on bacterial adhesion depends heavily on the scale of the topographical features. At the macroscopic level, unintentional roughness—often an inherent byproduct of geometrical complexity, extrusion limitations, or partially melted powder in 3D-printed architectures—creates microscopic grooves and crevices that actively shelter adherent bacteria. Notably, in SLM of titanium alloys, a smoother, unfavorable profile for bacteria can be achieved directly by rationally optimizing the build inclination angle. Lowering the build angle significantly minimizes the adherence of partially melted titanium particles, thereby eliminating these protective crevices and restricting *S. aureus* biofilm coverage.[165] Conversely, purposefully engineered submicron roughness can exert a potent antimicrobial effect by physically disrupting bacterial attachment. For example, the incorporation of submicron silicon nitride powders into polymer filaments (e.g., polyetheretherketone [PEEK]) for FFF generates a uniformly uneven surface topography. Unlike random manufacturing defects, this targeted micro-roughness restricts the spatial footprint available for bacteria, significantly impeding colonization (demonstrating up to a 94% reduction in *Staphylococcus epidermidis* and *E. coli* adhesion).[166]

At the nanoscale, biomimetic topographies inspired by nature (e.g., lotus leaves and dragonfly wings) exert potent "mechanobactericidal" effects. Various nanotextured structures—including nano-spikes (N4), nano-daggers (N2), nano-spinules (N1), and flame-like features (N5)—can be fabricated on Ti surfaces via single-step, cost-effective electrochemical anodization.[167] Their antimicrobial efficacy depends critically on three morphological

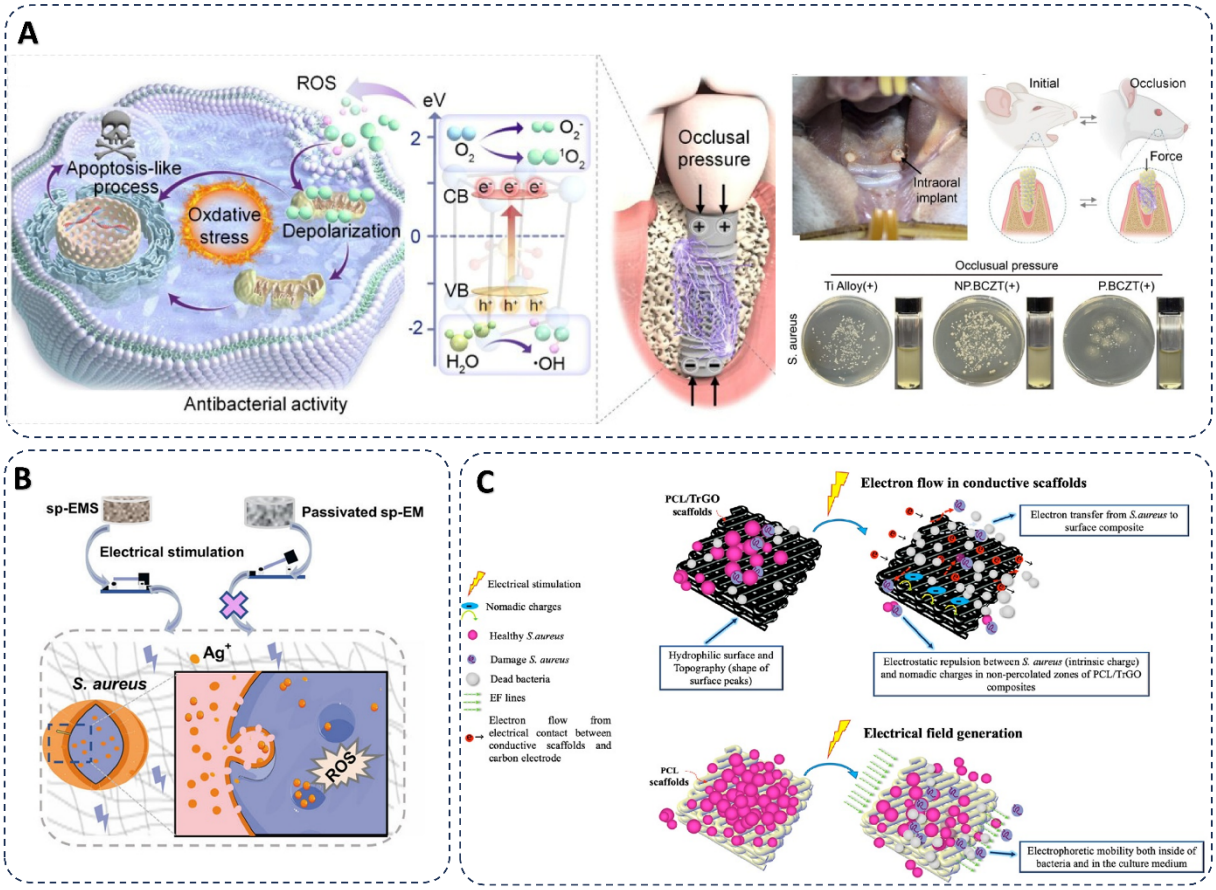

Figure 11. Representative electro-responsive and electroactive antimicrobial strategies in 3D-printed scaffolds. (A) Design and mechanism of an occlusion-activated autonomous piezoelectric dental implant. Daily masticatory forces mechanically trigger a built-in electric field, generating abundant reactive oxygen species (ROS) to eradicate peri-implantitis-associated pathogens. Reprinted from Chen *et al.*[16] (B) Mechanistic overview of a self-promoted electroactive mineralized scaffold (sp-EMS). Reprinted from Li *et al.*[17] (C) Proposed antibacterial pathways of a 3D-printed polycaprolactone/thermally reduced graphene oxide (PCL/TrGO) composite. Exogenous electrical stimulation significantly amplifies the scaffold's intrinsic bactericidal activity via electron transfer and cellular membrane disruption. Reprinted from Angulo-Pineda *et al.*[42]

parameters: size, shape, and spacing. Sharp high-aspect-ratio structures (e.g., N1, N4) function as physical nanocatalysts that puncture bacterial cell membranes upon contact, resulting in the fatal leakage of intracellular contents.[167] Conversely, concave or differently spaced structures (e.g., papillae, N3) mechanically constrain the spatial footprint available for bacterial attachment, thereby preventing bacterial aggregation. Furthermore, because purely physical nanostructures can sometimes exhibit limited efficacy against Gram-positive bacteria possessing thicker peptidoglycan layers, recent advancements have sought to intimately combine physical and chemical bactericidal mechanisms. For example, cicada-inspired fluoridated HA nanostructured surfaces, synthesized via electrochemical AM, synergistically couple the mechanical puncturing effect of nanopillars with the localized chemical toxicity of released fluorine ions, significantly enhancing broad-spectrum bacterial eradication.[168] Moreover, to maximize both antimicrobial and osteogenic potential, researchers have engineered hierarchical dual micro- to nano-topographies.[169] By combining SLM with sequential electrochemical anodization and hydrothermal treatments, Ti alloy surfaces can be designed to feature SLM-derived microparticles uniformly sheathed in vertically aligned titanate nanopillars. This bioinspired dual architecture effectively acts as a mechanical "bed of nails" to rupture pathogenic membranes while simultaneously promoting robust osteoblast adhesion and mineralisation[170] (Figure 12).

Despite these promising mechanobactericidal capabilities, the clinical translation of engineered surface structures faces several formidable challenges. First, the

underlying mechanisms involve complex, incompletely understood interactions among surface morphology, wettability, and chemical composition. Second, there is a persistent "race for the surface" trade-off: while certain highly hydrophobic nanotextured structures (e.g., N4, N5) effectively physically repel or rupture bacteria, their reduced hydrophilicity simultaneously impairs initial osteoblast adhesion, proliferation, and subsequent osseointegration.[167] Similarly, highly porous architectures may resist biofilm formation, but risk compromising the scaffold's load-bearing mechanical integrity. Finally, fabricating these specialized hierarchical topographies demands sophisticated, multi-step manufacturing processes. For Ti alloy implants, engineering a complete dual micro- to nano-topography typically requires coupling SLM with post-processing techniques such as electrochemical anodization and hydrothermal treatments.[170] This procedural complexity not only significantly elevates production costs but also complicates rigorous quality assurance, challenging consistent, large-scale reproduction of optimal surface characteristics.

To fully realize the potential of these engineered topographies, future research must prioritize: (i) elucidating the fundamental mechanobactericidal mechanisms at the bio-interface to optimize surface designs; (ii) simplifying 3D printing processes to ensure cost-effective scalability; and (iii) expanding rigorous *in vivo* clinical validation. These advancements will accelerate the bench-to-bedside adoption of 3D-printed implants with engineered surface structures, ultimately improving treatment outcomes while minimizing infection risks and patient complications.

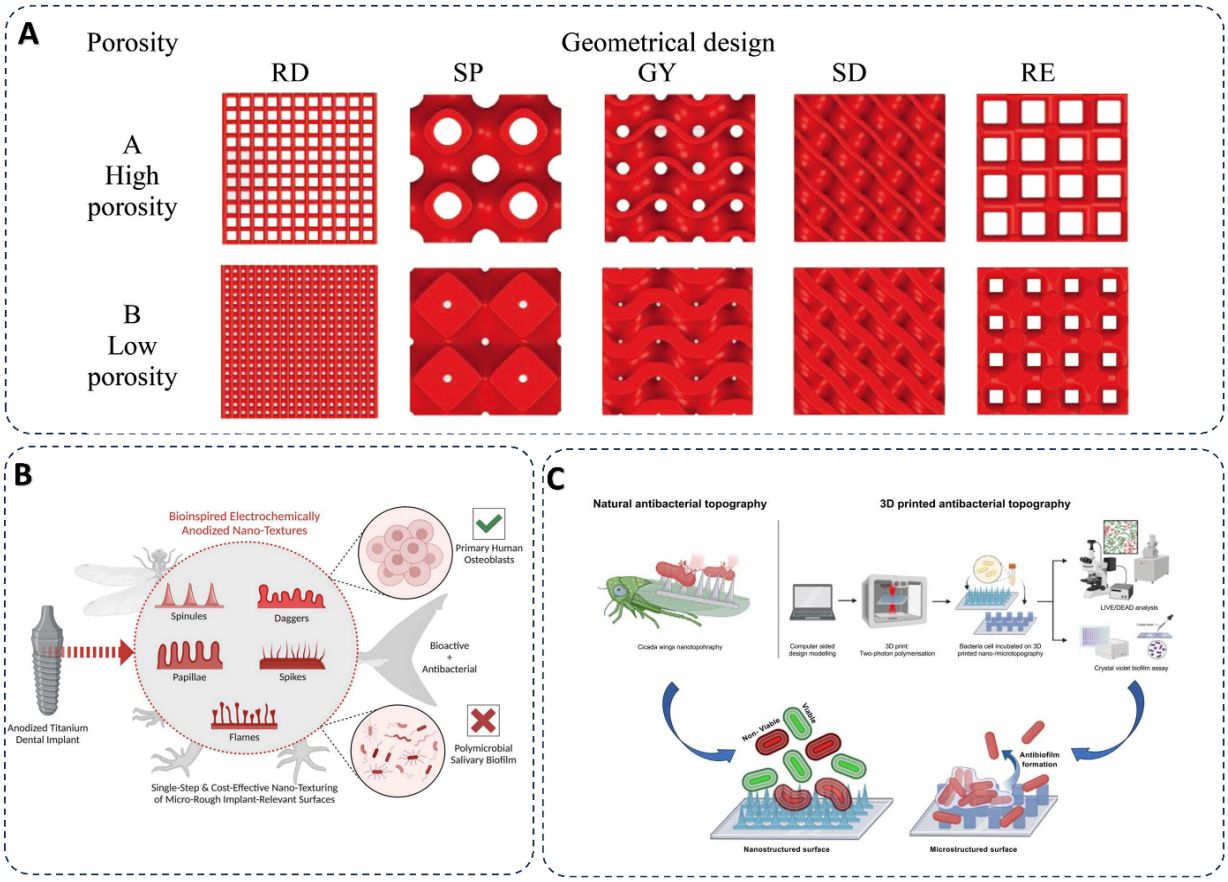

Figure 12. Representative structural and topographical antimicrobial strategies for 3D-printed implants. (A) Macro-scale architectural design. Varying 3D-printed scaffold geometries and porosities inherently restrict stable bacterial attachment and subsequent biofilm formation. Reprinted from Al-Tamimi *et al.*[163] (B) Nanoscale surface engineering. Purposefully designed nanotextures mechanically rupture bacterial membranes upon contact, conferring potent antimicrobial efficacy. Reprinted from Chopra *et al.*[167] (C) Bioinspired hierarchical topographies. Nature-derived nano- and micro-architectures exert durable, drug-free mechanobactericidal effects. Reprinted from Tan *et al.*[169]
Abbreviations: GY: Gyroid; RD: Reference design; RE: Re-entrant auxetic; SD: Schwarz diamond; SP: Schwarz primitive.

5. Conclusion

The advent of 3D printing has transformed the design and fabrication of medical implants, enabling unprecedented structural customization and anatomical precision. Nevertheless, the persistent burden of implant-associated infections underscores the need for a paradigm shift from conventional bioinert scaffolds towards advanced, multifunctional antimicrobial constructs. This review has systematically explored the potential of three principal antimicrobial strategies within 3D printing: intrinsic antibacterial biomaterials, stimuli-responsive systems, and bio-inspired structural micro-architectures.

Despite notable progress, each approach is accompanied by distinct translational and manufacturing hurdles. Intrinsic materials—particularly metal-based formulations—necessitate a delicate equilibrium between sustained bactericidal ion release and the mitigation of long-term mammalian cytotoxicity. Stimuli-responsive platforms enable spatiotemporal control over deep-tissue infections; however, their implementation frequently entails specialized external instrumentation and tailored clinical workflows. Topographical microstructuring offers a chemical-free antimicrobial mechanism but remains constrained by unresolved fabrication complexities and the inherent tension between bacterial inhibition and host cell osseointegration.

Looking ahead, next-generation 3D-printed scaffolds are anticipated to increasingly leverage the synergistic integration of these modalities. Future design paradigms are expected to orchestrate mechanobactericidal surface topographies in concert with stimuli-responsive materials, thereby achieving both on-demand infection eradication and sustained prophylactic function. Moreover, expediting the clinical translation of these technologies will necessitate a transition from simplified *in vitro* models to rigorous, long-term *in vivo* assessments conducted in physiologically relevant infected defect models. Such investigations are critical to delineating the dynamic interplay among bactericidal efficacy, material degradation kinetics, and host immune responses, ultimately informing the rational development of anti-infective implants with enhanced therapeutic and translational outcomes.

Acknowledgments

None.

Funding

This work was supported by the National Key Research and Development Program (China, grant 2023YFB4604700), the National Natural Science Foundation (China, grant 52475355), and the Key Project of the Interdisciplinary Research Support Program of Huazhong University of Science and Technology (grant 2025JCYJ037).

Conflict of Interest

The authors declare no conflict of interest.

Author contributions

Conceptualization: Zhixiang Nie, Yunsong Shi
Funding acquisition: Yunsong Shi
Project administration: Yunsong Shi
Supervision: Ke Li, Yuhuai Liao, Zhiyao Zhang
Writing–original draft: Zhixiang Nie, Zihan Qu, Shujing Wu, Yixuan Chen
Writing–review & editing: Zhixiang Nie, Zihan Qu, Lanyang Liu

Ethics approval and consent to participate

Not applicable.

Consent for publication

Not applicable.

Availability of data

Not applicable.

References

1. Lee SJ, Jeong W, Atala A. 3D Bioprinting for Engineered Tissue Constructs and Patient-Specific Models: Current Progress and Prospects in Clinical Applications. *Adv Mater.* 2024;36(49):2408032.

   doi: 10.1002/adma.202408032

2. Wu D, Zhu DC, Zhou XY, *et al*. Development of Intervertebral Disc Organoids through Directed Differentiation of Mesenchymal Stem Cells and Hierarchical 3D Printing. *ACS Nano.* 2026;20(12):9619-9637.

   doi: 10.1021/acsnano.5c14391

3. Zhang LJ, Yang YR, Xiong YH, *et al*. Infection-responsive long-term antibacterial bone plates for open fracture therapy. *Bioact Mater.* 2023;25:1-12.

   doi: 10.1016/j.bioactmat.2023.01.002

4. de la Fuente-Nunez C, Cesaro A, Hancock REW. Antibiotic failure: Beyond antimicrobial resistance. *Drug Resist Updat.* 2023;71:101012.

   doi: 10.1016/j.drup.2023.101012

5. Liu X, Lu S, Wang T, Wang X, Yang K, Yang H. Advances and prospects of 3D printed antibacterial bone implants: A systematic review. *J Mater Sci Technol.* 2024;200:227-242.

doi: 10.1016/j.jmst.2024.02.040

6. Qu X, Wang M, Wang M, *et al*. Multi-Mode Antibacterial Strategies Enabled by Gene-Transfection and Immunomodulatory Nanoparticles in 3D-Printed Scaffolds for Synergistic Exogenous and Endogenous Treatment of Infections. *Adv Mater.* 2022;34(18):e2200096.

   doi: 10.1002/adma.202200096

7. Zhang S, Shi XT, Miao ZY, *et al*. 3D-Printed Polyurethane Tissue-Engineering Scaffold with Hierarchical Microcellular Foam Structure and Antibacterial Properties. *Adv Eng Mater.* 2022;24(3):2101134.

   doi: 10.1002/adem.202101134

8. Li Z, Zhao Y, Wang Z, *et al*. Engineering Multifunctional Hydrogel-Integrated 3D Printed Bioactive Prosthetic Interfaces for Osteoporotic Osseointegration. *Adv Healthc Mater.* 2022;11(11):e2102535.

   doi: 10.1002/adhm.202102535

9. Alizadehgiashi M, Nemr CR, Chekini M, *et al*. Multifunctional 3D-Printed Wound Dressings. *ACS Nano.* 2021;15(7):12375-12387.

   doi: 10.1021/acsnano.1c04499

10. Xiao Y, Ding Y, Qiu J, *et al*. Treatment effects of 3D-printed PCL/Fe3O4@ZIF-8 magnetic nanocomposite on infected bone defect. *Int J Bioprint.* 2024;10(4):2271.

    doi: 10.36922/ijb.2271

11. Li WH, Zhong JT, Wang X, *et al*. Intelligent Responsive Zeolitic Imidazolate Framework-8@Copper Oxide Nanocomposite 3D-Printed Scaffolds for Efficient Repair of Infected Bone Defects. *ACS Nano.* 2025;19(39):35154-35180.

    doi: 10.1021/acsnano.5c13201

12. Rybak D, Du JT, Nakielski P, *et al*. NIR-Light Activable 3D Printed Platform Nanoarchitectured with Electrospun Plasmonic Filaments for On Demand Treatment of Infected Wounds. *Adv Healthc Mater.* 2025;14(6):2404274.

    doi: 10.1002/adhm.202404274

13. Tang XX, Chen XL, Zhang SM, *et al*. Silk-Inspired In Situ Hydrogel with Anti-Tumor Immunity Enhanced Photodynamic Therapy for Melanoma and Infected Wound Healing. *Adv Funct Mater.* 2021;31(17):2101320.

    doi: 10.1002/adfm.202101320

14. Huang Y, Wan X, Su Q, *et al*. Ultrasound-activated piezo-hot carriers trigger tandem catalysis coordinating cuproptosis-like bacterial death against implant infections. *Nat Commun.* 2024;15(1):1643.

    doi: 10.1038/s41467-024-45619-y

15. Pan QY, Zheng Y, Zhou Y, *et al*. Doping Engineering of Piezo-Sonocatalytic Nanocoating Confer Dental Implants with Enhanced Antibacterial Performances and Osteogenic Activity. *Adv Funct Mater.* 2024;34(21):2313553.

    doi: 10.1002/adfm.202313553

16. Chen A, Li K, Li Y, *et al*. Occlusion-activated autonomous piezoelectric implants for adaptive prevention of peri-implantitis. *Nat Commun.* 2026;17:5017.

    doi: 10.1038/s41467-026-71556-z

17. Li Z, He D, Guo B, *et al*. Self-promoted electroactive biomimetic mineralized scaffolds for bacteria-infected bone regeneration. *Nat Commun.* 2023;14(1):6963.

    doi: 10.1038/s41467-023-42598-4

18. Tang X, Ji X, Zhang R, Xu N, Feng Y, Pan L. Preparation and properties of a green material: a seawater degradable polyglycolic acid (PGA)/chitosan (CS) antibacterial composite material. *Int J Biol Macromol.* 2025;318(Pt 2):144993.

    doi: 10.1016/j.ijbiomac.2025.144993

19. Wang YX, Wang ZC, Lu WY, Hu Y. Review on chitosan-based antibacterial hydrogels: Preparation, mechanisms, and applications. *Int J Biol Macromol.* 2024;255:128080.

    doi: 10.1016/j.ijbiomac.2023.128080

20. Zhao D, Dong H, Niu Y, *et al*. Electrophoretic deposition of novel semi-permeable coatings on 3D-printed Ti-Nb alloy meshes for guided alveolar bone regeneration. *Dent Mater.* 2022;38(2):431-443.

    doi: 10.1016/j.dental.2021.12.026

21. Zhang X, Cheng F, Islam MR, Li HB. The fabrication of the chitosan-based bioink for in vitro tissue repair and regeneration: A review. *Int J Biol Macromol.* 2024;257:128504.

    doi: 10.1016/j.ijbiomac.2023.128504

22. Cabral CSD, Miguel SP, de Melo-Diogo D, Louro RO, Correia IJ. Green reduced graphene oxide functionalized 3D printed scaffolds for bone tissue regeneration. *Carbon.* 2019;146:513-523.

    doi: 10.1016/j.carbon.2019.01.100

23. Kaçoglu HS, Ceylan Ö, Çelebi M. Comparative study of the effect of cross-linking degree on chitosan hydrogels synthesized with low and medium molecular weight chitosan. *Polym Eng Sci.* 2024;64(3):1326-1339.

    doi: 10.1002/pen.26619

24. Yang Y, Yang S, Wang Y, *et al*. Anti-infective efficacy, cytocompatibility and biocompatibility of a 3D-printed osteoconductive composite scaffold functionalized with quaternized chitosan. *Acta Biomater.* 2016;46:112-128.

    doi: 10.1016/j.actbio.2016.09.035

25. Chen XY, Zhou YQ, Zhou SQ, *et al*. 3D printing of chitosan hydrogel reinforced with tubular nanoclay for hemostasis and infected wound healing. *Bioact Mater.* 2025;54:404-422.

doi: 10.1016/j.bioactmat.2025.08.024

26. Wang C, Hong T, Cui P, Wang J, Xia J. Antimicrobial peptides towards clinical application: Delivery and formulation. *Adv Drug Deliv Rev.* 2021;175:113818.

doi: 10.1016/j.addr.2021.05.028

27. Zhang QY, Yan ZB, Meng YM, *et al*. Antimicrobial peptides: mechanism of action, activity and clinical potential. *Mil Med Res.* 2021;8(1):48.

doi: 10.1186/s40779-021-00343-2

28. Li MM, Zhao PZ, Wang JW, Zhang XC, Li J. Functional antimicrobial peptide-loaded 3D scaffolds for infected bone defect treatment with AI and multidimensional printing. *Mater Horiz.* 2025;12(1):20-36.

doi: 10.1039/d4mh01124d

29. Gao XH, Ding JQ, Liao CB, Xu JL, Liu XX, Lu WY. Defensins: The natural peptide antibiotic. *Adv Drug Deliv Rev.* 2021;179:114008.

doi: 10.1016/j.addr.2021.114008

30. Nagaoka I, Tamura H, Reich J. Therapeutic Potential of Cathelicidin Peptide LL-37, an Antimicrobial Agent, in a Murine Sepsis Model. *Int J Mol Sci.* 2020;21(17):5973.

doi: 10.3390/ijms21175973

31. Li X, Huang X, Li L, *et al*. LL-37-Coupled Porous Composite Scaffold for the Treatment of Infected Segmental Bone Defect. *Pharmaceutics.* 2022;15(1):88.

doi: 10.3390/pharmaceutics15010088

32. Hu W, Peng C, Luo W, *et al*. Graphene-Based Antibacterial Paper. *ACS Nano.* 2010;4(7):4317-4323.

doi: 10.1021/nn101097v

33. Tashan H, Khosravi-Darani K, Yazdian F, *et al*. Antibacterial Properties of Graphene Based Nanomaterials: An Emphasis on Molecular Mechanisms, Surface Engineering and Size of Sheets. *Mini-Rev Org Chem.* 2019;16(2):159-172.

doi: 10.2174/1570193x15666180712120309

34. Pham VTH, Truong VK, Quinn MDJ, *et al*. Graphene Induces Formation of Pores That Kill Spherical and Rod-Shaped Bacteria. *ACS Nano.* 2015;9(8):8458-8467.

doi: 10.1021/acsnano.5b03368

35. Perreault F, de Faria AF, Nejati S, Elimelech M. Antimicrobial Properties of Graphene Oxide Nanosheets: Why Size Matters. *ACS Nano.* 2015;9(7):7226-7236.

doi: 10.1021/acsnano.5b02067

36. Zou X, Zhang L, Wang Z, Luo Y. Mechanisms of the Antimicrobial Activities of Graphene Materials. *J Am Chem Soc.* 2016;138(7):2064-2077.

doi: 10.1021/jacs.5b11411

37. Jia Z, Shi Y, Xiong P, *et al*. From Solution to Biointerface: Graphene Self-Assemblies of Varying Lateral Sizes and Surface Properties for Biofilm Control and Osteodifferentiation. *ACS Appl Mater Interfaces.* 2016;8(27):17151-17165.

doi: 10.1021/acsami.6b05198

38. Hegab HM, ElMekawy A, Zou L, Mulcahy D, Saint CP, Ginic-Markovic M. The controversial antibacterial activity of graphene-based materials. *Carbon.* 2016;105:362-376.

doi: 10.1016/j.carbon.2016.04.046

39. An X, Ma H, Liu B, Wang J, Yan X. Graphene Oxide Reinforced Polylactic Acid/Polyurethane Antibacterial Composites. *J Nanomater.* 2013;2013(1).

doi: 10.1155/2013/373414

40. Lu B, Li T, Zhao H, *et al*. Graphene-based composite materials beneficial to wound healing. *Nanoscale.* 2012;4(9):2978-2982.

doi: 10.1039/c2nr11958g

41. Nie R, Sun Y, Lv H, *et al*. 3D printing of MXene composite hydrogel scaffolds for photothermal antibacterial activity and bone regeneration in infected bone defect models. *Nanoscale.* 2022;14(22):8112-8129.

doi: 10.1039/d2nr02176e

42. Angulo-Pineda C, Srirussamee K, Palma P, Fuenzalida VM, Cartmell SH, Palza H. Electroactive 3D Printed Scaffolds Based on Percolated Composites of Polycaprolactone With Thermally Reduced Graphene Oxide for Antibacterial and Tissue Engineering Applications. *Nanomaterials.* 2020;10(3):428.

doi: 10.3390/nano10030428

43. Melo SF, Neves SC, Pereira AT, *et al*. Incorporation of graphene oxide into poly(ε-caprolactone) 3D printed fibrous scaffolds improves their antimicrobial properties. *Mater Sci Eng C.* 2020;109:110537.

doi: 10.1016/j.msec.2019.110537

44. Gomes RN, Borges I, Pereira AT, *et al*. Antimicrobial graphene nanoplatelets coatings for silicone catheters. *Carbon.* 2018;139:635-647.

doi: 10.1016/j.carbon.2018.06.044

45. Pinto AM, Gonçalves C, Sousa DM, *et al*. Smaller particle size and higher oxidation improves biocompatibility of graphene-based materials. *Carbon.* 2016;99:318-329.

doi: 10.1016/j.carbon.2015.11.076

46. Tao B, Chen M, Lin C, *et al*. Zn-incorporation with graphene oxide on Ti substrates surface to improve osteogenic activity and inhibit bacterial adhesion. *J Biomed Mater Res A.* 2019;107(10):2310-2326.

doi: 10.1002/jbm.a.36740

47. Cometta S, Donose BC, Juárez-Saldivar A, *et al*. Unravelling the physicochemical and antimicrobial mechanisms of

human serum albumin/tannic acid coatings for medical-grade polycaprolactone scaffolds. *Bioact Mater.* 2024;42:68-84.

doi: 10.1016/j.bioactmat.2024.08.023

48. Zhou W, Jia Z, Xiong P, *et al*. Bioinspired and Biomimetic AgNPs/Gentamicin-Embedded Silk Fibroin Coatings for Robust Antibacterial and Osteogenetic Applications. *ACS Appl Mater Interfaces.* 2017;9(31):25830-25846.

doi: 10.1021/acsami.7b06757

49. Smith JL, Tran N, Song T, Liang D, Qian M. Robust bulk micro-nano hierarchical copper structures possessing exceptional bactericidal efficacy. *Biomaterials.* 2022;280:121271.

doi: 10.1016/j.biomaterials.2021.121271

50. Qian J, Chen Y, Zhang W, *et al*. Micro/Nano-Structured Metal-Organic/Inorganic Hybrid Coatings on Biodegradable Zn for Osteogenic and Biocompatible Improvement. *Adv Mater Interfaces.* 2022;9(6).

doi: 10.1002/admi.202101852

51. Wang C, Zhang B, Yu S, *et al*. Incorporation of Mg-phenolic networks as a protective coating for magnesium alloy to enhance corrosion resistance and osteogenesis in vivo. *J Magnesium Alloys.* 2023;11(11):4247-4262.

doi: 10.1016/j.jma.2022.03.010

52. Perdikaki A, Galeou A, Pilatos G, *et al*. Ag and Cu Monometallic and Ag/Cu Bimetallic Nanoparticle-Graphene Composites with Enhanced Antibacterial Performance. *ACS Appl Mater Interfaces.* 2016;8(41):27498-27510.

doi: 10.1021/acsami.6b08403

53. Pham DQ, Gangadoo S, Berndt CC, *et al*. Antibacterial Longevity of a Novel Gallium Liquid Metal/Hydroxyapatite Composite Coating Fabricated by Plasma Spray. *ACS Appl Mater Interfaces.* 2022;14(16):18974-18988.

doi: 10.1021/acsami.2c03695

54. Han J, Ma Q, An Y, *et al*. The current status of stimuli-responsive nanotechnologies on orthopedic titanium implant surfaces. *J Nanobiotechnology.* 2023;21(1):277.

doi: 10.1186/s12951-023-02017-8

55. Jia B, Zhang Z, Zhuang Y, *et al*. High-strength biodegradable zinc alloy implants with antibacterial and osteogenic properties for the treatment of MRSA-induced rat osteomyelitis. *Biomaterials.* 2022;287:121663.

doi: 10.1016/j.biomaterials.2022.121663

56. Zhang E, Zhao X, Hu J, Wang R, Fu S, Qin G. Antibacterial metals and alloys for potential biomedical implants. *Bioact Mater.* 2021;6(8):2569-2612.

doi: 10.1016/j.bioactmat.2021.01.030

57. Chen Y, Li WL, Zhang C, Wu ZY, Liu J. Recent Developments of Biomaterials for Additive Manufacturing of Bone Scaffolds. *Adv Healthc Mater.* 2020;9(23):2000724.

doi: 10.1002/adhm.202000724

58. Alam F, Shukla VR, Varadarajan KM, Kumar S. Microarchitected 3D printed polylactic acid (PLA) nanocomposite scaffolds for biomedical applications. *J Mech Behav Biomed Mater.* 2020;103:103576.

doi: 10.1016/j.jmbbm.2019.103576

59. Maharubin S, Hu Y, Sooriyaarachchi D, Cong W, Tan GZ. Laser engineered net shaping of antimicrobial and biocompatible titanium-silver alloys. *Mater Sci Eng C.* 2019;105:110059.

doi: 10.1016/j.msec.2019.110059

60. Arjunan A, Robinson J, Al Ani E, Heaselgrave W, Baroutaji A, Wang C. Mechanical performance of additively manufactured pure silver antibacterial bone scaffolds. *J Mech Behav Biomed Mater.* 2020;112:104090.

doi: 10.1016/j.jmbbm.2020.104090

61. Marsh AC, Zhang Y, Poli L, *et al*. 3D printed bioactive and antibacterial silicate glass-ceramic scaffold by fused filament fabrication. *Mater Sci Eng C.* 2021;118:111516.

doi: 10.1016/j.msec.2020.111516

62. Qing Y, Li K, Li D, Qin Y. Antibacterial effects of silver incorporated zeolite coatings on 3D printed porous stainless steels. *Mater Sci Eng C.* 2020;108:110430.

doi: 10.1016/j.msec.2019.110430

63. Jia Z, Xiu P, Xiong P, *et al*. Additively Manufactured Macroporous Titanium with Silver-Releasing Micro-/Nanoporous Surface for Multipurpose Infection Control and Bone Repair - A Proof of Concept. *ACS Appl Mater Interfaces.* 2016;8(42):28495-28510.

doi: 10.1021/acsami.6b10473

64. Li JY, Li LL, Zhou J, *et al*. 3D printed dual-functional biomaterial with self-assembly micro-nano surface and enriched nano argentum for antibacterial and bone regeneration. *Appl Mater Today.* 2019;17:206-215.

doi: 10.1016/j.apmt.2019.06.012

65. Qiao SC, Wu DL, Li ZH, *et al*. The combination of multi-functional ingredients-loaded hydrogels and three-dimensional printed porous titanium alloys for infective bone defect treatment. *J Tissue Eng.* 2020;11:2041731420965797.

doi: 10.1177/2041731420965797

66. Bu LT, Wei X, Zhang YX, *et al*. Gradient 3D printed PEEK with nano-coating facilitates rapid manufacturing with dual enhanced osteogenic and anti-bacterial property. *Mater Today Bio.* 2025;35:102432.

doi: 10.1016/j.mtbio.2025.102432

67. Ciliveri S, Bandyopadhyay A. Enhanced osteogenesis

and bactericidal performance of additively manufactured MgO- and Cu-added CpTi for load-bearing implants. *Int J Bioprint.* 2023;9(6):552-565.

doi: 10.36922/ijb.1167

68. Gao JB, Jin YT, Fan YQ, *et al*. Fabricating antibacterial CoCrCuFeNi high-entropy alloy via selective laser melting and in-situ alloying. *J Mater Sci Technol.* 2022;102:159-165.

doi: 10.1016/j.jmst.2021.07.002

69. Wang B, Shan XH, Gao JY, *et al*. 3D-Printed Hydrogel Patches Embedded with Cu-Modified Liquid Metal Nanoparticles for Accelerated Wound Healing. *Adv Healthc Mater.* 2025;14(15):2404986.

doi: 10.1002/adhm.202404986

70. Liang YJ, Dai JB, Zhang ZB, *et al*. Osteogenic and antibacterial enhancement by alloying design and microstructural modification of additively manufactured biodegradable metals. *Biomaterials.* 2026;324:123481.

doi: 10.1016/j.biomaterials.2025.123481

71. Zou F, Jiang JY, Lv FZ, Xia XL, Ma XS. Preparation of antibacterial and osteoconductive 3D-printed PLGA/Cu(I)@ZIF-8 nanocomposite scaffolds for infected bone repair. *J Nanobiotechnol.* 2020;18(1):39.

doi: 10.1186/s12951-020-00594-6

72. Xie K, Wang N, Guo Y, *et al*. Additively manufactured biodegradable porous magnesium implants for elimination of implant-related infections: An in vitro and in vivo study. *Bioact Mater.* 2022;8:140-152.

doi: 10.1016/j.bioactmat.2021.06.032

73. Cockerill I, Su Y, Sinha S, *et al*. Porous zinc scaffolds for bone tissue engineering applications: A novel additive manufacturing and casting approach. *Mater Sci Eng C.* 2020;110:110738.

doi: 10.1016/j.msec.2020.110738

74. Yang Y, Yang M, He C, *et al*. Rare earth improves strength and creep resistance of additively manufactured Zn implants. *Compos B Eng.* 2021;216:108882.

doi: 10.1016/j.compositesb.2021.108882

75. Bhattacharjee A, Bose S. 3D printed hydroxyapatite-Zn2+ functionalized starch composite bone grafts for orthopedic and dental applications. *Mater Des.* 2022;221:110903.

doi: 10.1016/j.matdes.2022.110903

76. Kodama J, Chen H, Zhou T, *et al*. Antibacterial efficacy of quaternized chitosan coating on 3D printed titanium cage in rat intervertebral disc space. *Spine J.* 2021;21(7):1217-1228.

doi: 10.1016/j.spinee.2021.02.016

77. Sanchez-Salcedo S, Garcia A, Gonzalez-Jimenez A, Vallet-Regi M. Antibacterial effect of 3D printed mesoporous bioactive glass scaffolds doped with metallic silver nanoparticles. *Acta Biomater.* 2023;155:654-666.

doi: 10.1016/j.actbio.2022.10.045

78. Maharubin S, Zhou Y, Tan GZ. Development and Investigation on a Silver Nanoparticle-Incorporated Electrofiltration System for Biofouling Control. *IEEE Trans Nanotechnol.* 2018;17(5):948-954.

doi: 10.1109/tnano.2018.2832210

79. Tan Z, Xu G, Orndorff PE, Shirwaiker RA. Effects of Electrically Activated Silver-Titanium Implant System Design Parameters on Time-Kill Curves Against Staphylococcus aureus. *J Med Biol Eng.* 2016;36(3):325-333.

doi: 10.1007/s40846-016-0136-x

80. Lara HH, Garza-Treviño EN, Ixtepan-Turrent L, Singh DK. Silver nanoparticles are broad-spectrum bactericidal and virucidal compounds. *J Nanobiotechnol.* 2011;9(1):30.

doi: 10.1186/1477-3155-9-30

81. Tan Z, Havell EA, Orndorff PE, Shirwaiker RA. Antibacterial efficacy and cytotoxicity of low intensity direct current activated silver-titanium implant system prototype. *Biometals.* 2017;30(1):113-125.

doi: 10.1007/s10534-017-9993-1

82. Brandt O, Mildner M, Egger AE, *et al*. Nanoscalic silver possesses broad-spectrum antimicrobial activities and exhibits fewer toxicological side effects than silver sulfadiazine. *Nanomedicine.* 2012;8(4):478-488.

doi: 10.1016/j.nano.2011.07.005

83. Ding M, Zhang Y, Li X, *et al*. Simultaneous Biofilm Disruption, Bacterial Killing, and Inflammation Elimination for Wound Treatment Using Silver Embellished Polydopamine Nanoplatform. *Small.* 2024;20(36):e2400927.

doi: 10.1002/smll.202400927

84. Verma A, Shivalkar S, Sk MP, Samanta SK, Sahoo AK. Nanocomposite of Ag nanoparticles and catalytic fluorescent carbon dots for synergistic bactericidal activity through enhanced reactive oxygen species generation. *Nanotechnology.* 2020;31(40):405704.

doi: 10.1088/1361-6528/ab996f

85. Praveen AS, Arjunan A. Effect of nano-Al2O3 addition on the microstructure and erosion wear of HVOF sprayed NiCrSiB coatings. *Mater Res Express.* 2019;7(1):015006.

doi: 10.1088/2053-1591/ab5bda

86. Praveen AS, Arjunan A. Parametric optimisation of high-velocity oxy-fuel nickel-chromium-silicon-boron and aluminium-oxide coating to improve erosion wear resistance. *Mater Res Express.* 2019;6(9):0696560.

doi: 10.1088/2053-1591/ab301c

87. Chouirfa H, Bouloussa H, Migonney V, Falentin-Daudre C. Review of titanium surface modification techniques

and coatings for antibacterial applications. *Acta Biomater.* 2019;83:37-54.

doi: 10.1016/j.actbio.2018.10.036

88. Pandey A, Patel AK, S A, *et al*. Enhanced Tribological and Bacterial Resistance of Carbon Nanotube with Ceria- and Silver-Incorporated Hydroxyapatite Biocoating. *Nanomaterials.* 2018;8(6):363.

doi: 10.3390/nano8060363

89. Surmeneva MA, Sharonova AA, Chernousova S, *et al*. Incorporation of silver nanoparticles into magnetron-sputtered calcium phosphate layers on titanium as an antibacterial coating. *Colloids Surf B Biointerfaces.* 2017;156:104-113.

doi: 10.1016/j.colsurfb.2017.05.016

90. Batebi K, Abbasi Khazaei B, Afshar A. Characterization of sol-gel derived silver/fluor-hydroxyapatite composite coatings on titanium substrate. *Surf Coat Technol.* 2018;352:522-528.

doi: 10.1016/j.surfcoat.2018.08.021

91. Durdu S, Aktug SL, Korkmaz K, Yalcin E, Aktas S. Fabrication, characterization and in vitro properties of silver-incorporated TiO2 coatings on titanium by thermal evaporation and micro-arc oxidation. *Surf Coat Technol.* 2018;352:600-608.

doi: 10.1016/j.surfcoat.2018.08.050

92. Vaithilingam J, Kilsby S, Goodridge RD, Christie SDR, Edmondson S, Hague RJM. Immobilisation of an antibacterial drug to Ti6Al4V components fabricated using selective laser melting. *Appl Surf Sci.* 2014;314:642-654.

doi: 10.1016/j.apsusc.2014.06.014

93. Vikulova ES, Dorovskikh SI, Sergeevichev DS, *et al*. Combination of Noble Metal and Gold-Silver Nanoclusters as Enhanced Antibacterial Coatings for Ti-Based Medical Implants. *Int J Mol Sci.* 2025;26(24):11945.

doi: 10.3390/ijms262411945

94. Liang R, Xu Y, Zhao M, *et al*. Properties of silver contained coatings on CoCr alloys prepared by vacuum plasma spraying. *Mater Sci Eng C.* 2020;106:110156.

doi: 10.1016/j.msec.2019.110156

95. Wu X, Liu S, Chen K, *et al*. 3D printed chitosan-gelatine hydrogel coating on titanium alloy surface as biological fixation interface of artificial joint prosthesis. *Int J Biol Macromol.* 2021;182:669-679.

doi: 10.1016/j.ijbiomac.2021.04.046

96. Astaneh ME, Fereydouni N. Silver Nanoparticles in 3D Printing: A New Frontier in Wound Healing. *ACS Omega.* 2024;9(40):41107-41129.

doi: 10.1021/acsomega.4c04961

97. Noyce JO, Michels H, Keevil CW. Potential use of copper surfaces to reduce survival of epidemic meticillin-resistant Staphylococcus aureus in the healthcare environment. *J Hosp Infect.* 2006;63(3):289-297.

doi: 10.1016/j.jhin.2005.12.008

98. Wilks SA, Michels H, Keevil CW. The survival of Escherichia coli O157 on a range of metal surfaces. *Int J Food Microbiol.* 2005;105(3):445-454.

doi: 10.1016/j.ijfoodmicro.2005.04.021

99. Chai H, Guo L, Wang X, *et al*. Antibacterial effect of 317L stainless steel contained copper in prevention of implant-related infection in vitro and in vivo. *J Mater Sci Mater Med.* 2011;22(11):2525-2535.

doi: 10.1007/s10856-011-4427-z

100. Wu C, Zhou Y, Xu M, *et al*. Copper-containing mesoporous bioactive glass scaffolds with multifunctional properties of angiogenesis capacity, osteostimulation and antibacterial activity. *Biomaterials.* 2013;34(2):422-433.

doi: 10.1016/j.biomaterials.2012.09.066

101. Zhuang Y, Ren L, Zhang S, Wei X, Yang K, Dai K. Antibacterial effect of a copper-containing titanium alloy against implant-associated infection induced by methicillin-resistant Staphylococcus aureus. *Acta Biomater.* 2021;119:472-484.

doi: 10.1016/j.actbio.2020.10.026

102. Wu Y, Shi X, Wang J, *et al*. A surface metal ion-modified 3D-printed Ti-6Al-4V implant with direct and immunoregulatory antibacterial and osteogenic activity. *Front Bioeng Biotechnol.* 2023;11:1142264.

doi: 10.3389/fbioe.2023.1142264

103. Fathalla RK, Engel M, Ducho C. Targeting the binding pocket of the fluorophore 8-anilinonaphthalene-1-sulfonic acid in the bacterial enzyme MurA. *Arch Pharm.* 2023;356(9):2300237.

doi: 10.1002/ardp.202300237

104. Liu Y, Nie N, Tang H, *et al*. Effective Antibacterial Activity of Degradable Copper-Doped Phosphate-Based Glass Nanozymes. *ACS Appl Mater Interfaces.* 2021;13(10):11631-11645.

doi: 10.1021/acsami.0c22746

105. Shuai C, Pan G, Zhong Q, Peng S. Cu-S-Mo interfacial sites in CuO2@MoS2/PLLA scaffolds for robust synergistic antibacterial efficacy via CDT and PTT. *Surfaces Interfaces.* 2024;55:105432.

doi: 10.1016/j.surfin.2024.105432

106. Lakshminarayanan R, Ye E, Young DJ, Li Z, Loh XJ. Recent Advances in the Development of Antimicrobial Nanoparticles for Combating Resistant Pathogens. *Adv Healthc Mater.* 2018;7(13):e1701400.

doi: 10.1002/adhm.201701400

107. Liu AB, Zhang ZB, Wang X, *et al*. The critical role of surface characteristics in 3D-printed biodegradable Zn-based porous scaffolds for bone defect repair. *Virtual Phys Prototyp.* 2025;20(1):e2476035.

doi: 10.1080/17452759.2025.2476035

108. Chen K, Wang F, Sun X, *et al*. 3D-printed zinc oxide nanoparticles modified barium titanate/hydroxyapatite ultrasound-responsive piezoelectric ceramic composite scaffold for treating infected bone defects. *Bioact Mater.* 2025;45:479-495.

doi: 10.1016/j.bioactmat.2024.11.015

109. Qu X, Yang H, Jia B, Yu Z, Zheng Y, Dai K. Biodegradable Zn-Cu alloys show antibacterial activity against MRSA bone infection by inhibiting pathogen adhesion and biofilm formation. *Acta Biomater.* 2020;117:400-417.

doi: 10.1016/j.actbio.2020.09.041

110. Jiang X, Tang X, Zhang B, He L, Shi Y. Antimicrobial activity and synergistic antibacterial mechanism of a combination of zinc and rare-earth scandium against Escherichia coli. *Mater Technol.* 2019;35(11-12):797-806.

doi: 10.1080/10667857.2019.1688534

111. Yang Y, Cheng Y, Deng F, *et al*. A bifunctional bone scaffold combines osteogenesis and antibacterial activity via in situ grown hydroxyapatite and silver nanoparticles. *Bio-Des Manuf.* 2021;4(3):452-468.

doi: 10.1007/s42242-021-00130-x

112. Farias IAP, Dos Santos CCL, Sampaio FC. Antimicrobial Activity of Cerium Oxide Nanoparticles on Opportunistic Microorganisms: A Systematic Review. *Biomed Res Int.* 2018;2018:1923606.

doi: 10.1155/2018/1923606

113. Xia X, Song X, Li Y, *et al*. Antibacterial and anti-inflammatory ZIF-8@Rutin nanocomposite as an efficient agent for accelerating infected wound healing. *Front Bioeng Biotechnol.* 2022;10:1026743.

doi: 10.3389/fbioe.2022.1026743

114. Xu B, Wang H, Wang W, *et al*. A Single-Atom Nanozyme for Wound Disinfection Applications. *Angew Chem Int Ed Engl.* 2019;58(15):4911-4916.

doi: 10.1002/anie.201813994

115. Liu Y, Zheng Y, Chen XH, *et al*. Fundamental Theory of Biodegradable Metals—Definition, Criteria, and Design. *Adv Funct Mater.* 2019;29(18):1805402.

doi: 10.1002/adfm.201805402

116. Lee J, Byun H, Madhurakkat Perikamana SK, Lee S, Shin H. Current Advances in Immunomodulatory Biomaterials for Bone Regeneration. *Adv Healthc Mater.* 2019;8(4):e1801106.

doi: 10.1002/adhm.201801106

117. Nie ZX, Sun YS, Li K, *et al*. Non-destructive debridement and tuneable ion release via magnesium abrasion and electro-dissolution promote bone regeneration and osseointegration of infected implants. *Mater Today Bio.* 2026;38:103183.

doi: 10.1016/j.mtbio.2026.103183

118. Jiang M, Sun Y, Nie Z, *et al*. Cavitation erosion: An efficient method for promoting osteogenesis and immunomodulation of titanium surface. *Dent Mater.* 2025;41(11):1350-1360.

doi: 10.1016/j.dental.2025.07.017

119. Steijvers E, Shi YS, Lu H, *et al*. Rapid assessment of the osteogenic capacity of hydroxyapatite/aragonite using a murine tibial periosteal ossification model. *Bioact Mater.* 2025;45:257-273.

doi: 10.1016/j.bioactmat.2024.11.025

120. Shi YS, Tang SH, Yuan X, *et al*. In Situ 4D Printing of Polyelectrolyte/Magnetic Composites for Sutureless Gastric Perforation Sealing. *Adv Mater.* 2024;36(34):2307601.

doi: 10.1002/adma.202307601

121. Li Z, Zhang S, Wang Q, *et al*. Untethered & Stiffness-Tunable Ferromagnetic Liquid Robots for Cleaning Thrombus in Complex Blood Vessels. *Adv Mater.* 2024;36(46):e2409142.

doi: 10.1002/adma.202409142

122. Wang XX, Chen P, Yang H, *et al*. In Situ Imaging and Anti-inflammation of 3D Printed Scaffolds Enabled by AIEgen. *ACS Appl Mater Interfaces.* 2023;15(21):25382-25392.

doi: 10.1021/acsami.3c03082

123. Xue X, Zhang H, Liu H, *et al*. Rational Design of Multifunctional CuS Nanoparticle-PEG Composite Soft Hydrogel-Coated 3D Hard Polycaprolactone Scaffolds for Efficient Bone Regeneration. *Adv Funct Mater.* 2022;32(33):2202470.

doi: 10.1002/adfm.202202470

124. Wu Y, Liao Q, Wu L, *et al*. ZnL2-BPs Integrated Bone Scaffold under Sequential Photothermal Mediation: A Win-Win Strategy Delivering Antibacterial Therapy and Fostering Osteogenesis Thereafter. *ACS Nano.* 2021;15(11):17854-17869.

doi: 10.1021/acsnano.1c06062

125. He MM, Zhu C, Sun D, *et al*. Layer-by-layer assembled black phosphorus/chitosan composite coating for multi-functional PEEK bone scaffold. *Compos B Eng.* 2022;246:110266.

doi: 10.1016/j.compositesb.2022.110266

126. Liu WY, Zuo RT, Zhu TL, Zhu M, Zhao SC, Zhu YF. Forsterite-hydroxyapatite composite scaffolds with photothermal antibacterial activity for bone repair. *J Adv Ceram.* 2021;10(5):1095-1106.

doi: 10.1007/s40145-021-0494-x

127. Zhang L, Ng G, Kapoor-Kaushik N, *et al*. 2D Porphyrinic Metal-Organic Framework Nanosheets as Multidimensional Photocatalysts for Functional Materials. *Angew Chem Int Ed Engl.* 2021;60(42):22664-22671.

doi: 10.1002/anie.202107457

128. Wang Y, Frascella F, Gaglio CG, Pirri CF, Wei QF, Roppolo I. Vat Photopolymerization 3D Printing of Hydrogels Embedding Metal-Organic Frameworks for Photodynamic Antimicrobial Therapy. *ACS Appl Mater Interfaces.* 2024;16(42):57778-57791.

doi: 10.1021/acsami.4c15168

129. Sun XH, Xie SY, Fang Y, *et al*. A multimodal ROS logic-gated therapeutic platform disrupts the vicious cycle of senescence to promote aged bone defect repair. *Bioact Mater.* 2026;61:692-711.

doi: 10.1016/j.bioactmat.2026.02.002

130. Huang T, Sun Z, Heath DE, O'Brien-Simpson N, O'Connor AJ. 3D printed and smart alginate wound dressings with pH-responsive drug and nanoparticle release. *Chem Eng J.* 2024;492:152117.

doi: 10.1016/j.cej.2024.152117

131. Lin MY, Stehle Y, Chen L, *et al*. A 3D-printed chitosan-based pH-responsive dual functional scaffold for osteomyelitis: synergistic antibacterial and osteogenic treatment. *Carbohydr Polym.* 2025;366:123866.

doi: 10.1016/j.carbpol.2025.123866

132. Huo J, Jia Q, Huang H, *et al*. Emerging photothermal-derived multimodal synergistic therapy in combating bacterial infections. *Chem Soc Rev.* 2021;50(15):8762-8789.

doi: 10.1039/d1cs00074h

133. Fu S, Hu H, Chen J, Zhu Y, Zhao S. Silicone resin derived larnite/C scaffolds via 3D printing for potential tumor therapy and bone regeneration. *Chem Eng J.* 2020;382:122928.

doi: 10.1016/j.cej.2019.122928

134. Xie M, Zhu W, Yu KM, Zhu Z, Wang G. Effects of doping and rapid thermal processing in Y doped CdO thin films. *J Alloys Compd.* 2019;776:259-265.

doi: 10.1016/j.jallcom.2018.10.288

135. Li Y, Liu X, Li B, *et al*. Near-Infrared Light Triggered Phototherapy and Immunotherapy for Elimination of Methicillin-Resistant Staphylococcus aureus Biofilm Infection on Bone Implant. *ACS Nano.* 2020;14(7):8157-8170.

doi: 10.1021/acsnano.0c01486

136. Yang C, Luo Y, Lin H, Ge M, Shi J, Zhang X. Niobium Carbide MXene Augmented Medical Implant Elicits Bacterial Infection Elimination and Tissue Regeneration. *ACS Nano.* 2020;15(1):1086-1099.

doi: 10.1021/acsnano.0c08045

137. Gao Z, Song Z, Guo R, *et al*. Mn Single-Atom Nanozyme Functionalized 3D-Printed Bioceramic Scaffolds for Enhanced Antibacterial Activity and Bone Regeneration. *Adv Healthc Mater.* 2024;13(13):2303182.

doi: 10.1002/adhm.202303182

138. Park J, Jiang Q, Feng D, Mao L, Zhou H-C. Size-Controlled Synthesis of Porphyrinic Metal-Organic Framework and Functionalization for Targeted Photodynamic Therapy. *J Am Chem Soc.* 2016;138(10):3518-3525.

doi: 10.1021/jacs.6b00007

139. Wang C, Xie Z, deKrafft KE, Lin W. Doping Metal-Organic Frameworks for Water Oxidation, Carbon Dioxide Reduction, and Organic Photocatalysis. *J Am Chem Soc.* 2011;133(34):13445-13454.

doi: 10.1021/ja203564w

140. Meyer K, Ranocchiari M, van Bokhoven JA. Metal organic frameworks for photo-catalytic water splitting. *Energy Environ Sci.* 2015;8(7):1923-1937.

doi: 10.1039/C5EE00161G

141. He T, Ni B, Zhang S, *et al*. Ultrathin 2D Zirconium Metal-Organic Framework Nanosheets: Preparation and Application in Photocatalysis. *Small.* 2018;14(16):1703929.

doi: 10.1002/smll.201703929

142. Li JB, Wang Y, Fan L, *et al*. Liquid metal hybrid antibacterial hydrogel scaffolds from 3D printing for wound healing. *Chem Eng J.* 2024;496:153805.

doi: 10.1016/j.cej.2024.153805

143. Huang Y, Li J, Yu Z, Li J, Liang K, Deng Y. Elaborated Bio-Heterojunction With Robust Sterilization Effect for Infected Tissue Regeneration via Activating Competent Cell-Like Antibacterial Tactic. *Adv Mater.* 2024;36(48):e2414111.

doi: 10.1002/adma.202414111

144. Li X, Bai H, Yang Y, Yoon J, Wang S, Zhang X. Supramolecular Antibacterial Materials for Combatting Antibiotic Resistance. *Adv Mater.* 2019;31(5):e1805092.

doi: 10.1002/adma.201805092

145. Wang X, Zhong X, Bai L, *et al*. Ultrafine Titanium Monoxide (TiO1+x) Nanorods for Enhanced Sonodynamic Therapy. *J Am Chem Soc.* 2020;142(14):6527-6537.

doi: 10.1021/jacs.9b10228

146. Xu Y, Tang D, Li L, *et al*. A Bodipy-Based Aggregation-Induced Emission Nanoagent for Sonodynamic Antibacterial Studies. *Adv Funct Mater.* 2024;34(33):2315385.

doi: 10.1002/adfm.202315385

147. Lei C, Lei J, Zhang X, *et al*. Heterostructured piezocatalytic nanoparticles with enhanced ultrasound response for efficient repair of infectious bone defects. *Acta*

Biomater. 2023;172:343-354.

doi: 10.1016/j.actbio.2023.10.006

148. Wu C, Cheng K, Cheng J, *et al*. Reinforcing titanium surface modification through the integration of piezoelectric effect and structural design to mitigate early bacterial infection. *Ceram Int.* 2024;50(21):42645-42655.

doi: 10.1016/j.ceramint.2024.08.108

149. Chen Y, Wan X, Yue Y, *et al*. Low-Intensity Ultrasound-Activated Cavitation Effect Triggers Piezoelectric Catalysis Coordinating Respiratory Chain Interference Tactics Against Bacterial Infection. *Adv Funct Mater.* 2025;35(14):2419426.

doi: 10.1002/adfm.202419426

150. Zhao P, Li H, Bu W. A Forward Vision for Chemodynamic Therapy: Issues and Opportunities. *Angew Chem Int Ed Engl.* 2023;62(7):e202210415.

doi: 10.1002/anie.202210415

151. Duan Y, Yu Y, Liu P, *et al*. Reticular Chemistry-Enabled Sonodynamic Activity of Covalent Organic Frameworks for Nanodynamic Cancer Therapy. *Angew Chem Int Ed Engl.* 2023;62(20):e202302146.

doi: 10.1002/anie.202302146

152. Shi YS, Tang SH, Zhang WF, *et al*. A reliable, battery-free and implantable magnetic sensing system for wireless monitoring of spinal motion in rats and humans. *Chem Eng J.* 2024;482:148891.

doi: 10.1016/j.cej.2024.148891

153. Zeglio E, Rutz AL, Winkler TE, Malliaras GG, Herland A. Conjugated Polymers for Assessing and Controlling Biological Functions. *Adv Mater.* 2019;31(22):1806712.

doi: 10.1002/adma.201806712

154. Kiamco MM, Zmuda HM, Mohamed A, *et al*. Hypochlorous-Acid-Generating Electrochemical Scaffold for Treatment of Wound Biofilms. *Sci Rep.* 2019;9(1):2683.

doi: 10.1038/s41598-019-38968-y

155. Zituni D, Schütt-Gerowitt H, Kopp M, *et al*. The growth of Staphylococcus aureus and Escherichia coli in low-direct current electric fields. *Int J Oral Sci.* 2014;6(1):7-14.

doi: 10.1038/ijos.2013.64

156. Khan SI, Blumrosen G, Vecchio D, *et al*. Eradication of multidrug-resistant Pseudomonas biofilm with pulsed electric fields. *Biotechnol Bioeng.* 2016;113(3):643-650.

doi: 10.1002/bit.25818

157. Del Pozo JL, Rouse MS, Patel R. Bioelectric effect and bacterial biofilms. A systematic review. *Int J Artif Organs.* 2008;31(9):786-795.

doi: 10.1177/039139880803100906

158. Shi R, Zhang J, Tian J, *et al*. An effective self-powered strategy to endow titanium implant surface with associated activity of anti-biofilm and osteogenesis. *Nano Energy.* 2020;77:105201.

doi: 10.1016/j.nanoen.2020.105201

159. Chen X, Liu L, Feng Y, *et al*. Fluid eddy induced piezo-promoted photodegradation of organic dye pollutants in wastewater on ZnO nanorod arrays/3D Ni foam. *Mater Today.* 2017;20(9):501-506.

doi: 10.1016/j.mattod.2017.08.027

160. Chen A, Wang Z, Guan Z, *et al*. Echinoderm stereom gradient structures enable mechanoelectrical perception. *Nature.* 2026;651(8105):371-376.

doi: 10.1038/s41586-026-10164-9

161. Khare D, Basu B, Dubey AK. Electrical stimulation and piezoelectric biomaterials for bone tissue engineering applications. *Biomaterials.* 2020;258:120280.

doi: 10.1016/j.biomaterials.2020.120280

162. Akkineni AR, Spangenberg J, Geissler M, *et al*. Controlled and Local Delivery of Antibiotics by 3D Core/Shell Printed Hydrogel Scaffolds to Treat Soft Tissue Infections. *Pharmaceutics.* 2021;13(12):2151.

doi: 10.3390/pharmaceutics13122151

163. Al-Tamimi AA, Aldawood E. The effect of 3D-printed bone tissue scaffolds geometrical designs on bacterial biofilm formation. *Int J Bioprint.* 2024;10(1):1768.

doi: 10.36922/ijb.1768

164. Wang JG, Gao HC, Hu Y, *et al*. 3D printing of Pickering emulsion inks to construct poly(D,L-lactide-co-trimethylene carbonate)-based porous bioactive scaffolds with shape memory effect. *J Mater Sci.* 2021;56(1):731-745.

doi: 10.1007/s10853-020-05318-7

165. Avik S, Nhiem T, Aaqil R, *et al*. Rational design of additively manufactured Ti6Al4V implants to control Staphylococcus aureus biofilm formation. *Materialia.* 2019;5:100250.

doi: 10.1016/j.mtla.2019.100250

166. Basgul C, Desantis P, Derr T, Hickok NJ, Bock RM, Kurtz SM. Exploring the mechanical strength, antimicrobial performance, and bioactivity of 3D-printed silicon nitride-PEEK composites in cervical spinal cages. *Int J Bioprint.* 2024;10(2):431-444.

doi: 10.36922/ijb.2124

167. Chopra D, Guo TQ, Jayasree A, Gulati K, Ivanovski S. Bioinspired, Bioactive, and Bactericidal: Anodized Nanotextured Dental Implants. *Adv Funct Mater.* 2024;34(30):2314031.

doi: 10.1002/adfm.202314031

168. Ge X, Zhao JM, Esmeryan KD, *et al*. Cicada-inspired fluoridated hydroxyapatite nanostructured surfaces synthesized by electrochemical additive

manufacturing. *Mater Des.* 2020;193:108790.

doi: 10.1016/j.matdes.2020.108790

169. Tan N, Im J, Neate N, *et al*. Mechano-bactericidal activity of two-photon polymerized micro-and nanoscale topographies against Pseudomonas aeruginosa: Surface interactions and antibacterial efficacy. *Mater Today Commun.* 2024;40:109785.

doi: 10.1016/j.mtcomm.2024.109785

170. Maher S, Wijenayaka AR, Lima-Marques L, Yang DQ, Atkins GJ, Losic D. Advancing of Additive-Manufactured Titanium Implants with Bioinspired Micro- to Nanotopographies. *ACS Biomater Sci Eng.* 2021;7(2):441-450.

doi: 10.1021/acsbiomaterials.0c01210